

This paper develops a method of manipulating the squeezed atom state to generate a few-photon state whose phase or photon-number fluctuations are prescribed at our disposal. The squeezed atom state is a collective atomic state whose quantum fluctuations in population difference or collective dipole are smaller than those of the coherent atom state. It is shown that the squeezed atom state can be generated by the interaction of atoms with a coherent state of the electromagnetic field, and that it can be used as a tunable source of squeezed radiation. A variety of squeezed states, including the photon-number squeezed state and the phase squeezed state, can be produced by manipulating the atomic state. This is owing to the fact that quantum-statistical information of the atomic state is faithfully transferred to that of the photon state. Possible experimental situations to implement our theory are discussed.

42.50.Dv, 03.65.Bz, 42.50.Gy, 42.50.Lc

# Number-phase-squeezed few-photon state generated from squeezed atoms

Hiroki Saito and Masahito Ueda

*Department of Physical Electronics, Hiroshima University, Higashi-Hiroshima 739-8527, Japan  
and CREST, Japan Science and Technology Corporation (JST)*

## I. INTRODUCTION

Nonclassical properties and manipulation of the quantized electromagnetic (EM) field have been a center of interest in quantum optics [1]. A variety of methods have been proposed for the generation of squeezed states of the EM field, and several of them have been realized experimentally [2]. The quadrature-amplitude squeezed state in which fluctuations of the in-phase or out-of-phase component are suppressed to below those of the coherent state can be generated via nonlinear optical processes [3,4]. The photon-number squeezed state exhibiting sub-Poissonian photon statistics can be generated using semiconductor lasers [5], light-emitting diodes [6,7], and tailor-made semiconductor heterostructures [8].

A coherent state with average photon number  $\bar{n}$  has the relative photon-number fluctuation of  $\Delta n/\bar{n} = 1/\sqrt{\bar{n}}$  and the phase fluctuation of  $\Delta\phi \simeq 1/(2\sqrt{\bar{n}})$ . Hence, if  $\bar{n} \gg 1$ , there is practically no need of squeezing. In a few-photon regime, however,  $\Delta n$  becomes comparable to  $\bar{n}$  and  $\Delta\phi$  becomes of the order of one. It is thus within the few-photon regime that the manipulation of quantum fluctuations becomes crucially important. Such quantum-controlled few-photon states might be useful, e.g., for optical interconnections in semiconductor microstructures and spectroscopic diagnostics in biology.

In the present paper, we develop a method of manipulating a collective atomic state to generate quantum-controlled few-photon states [9]. Radiation from atoms has been extensively studied in quantum optics [10], e.g., superradiance [11], resonance fluorescence [12], photon emission in the cavity [13], etc. As regards nonclassical properties of radiation, it is known that resonant fluorescence exhibits photon anti-bunching and sub-Poissonian photon statistics [14,15]. It was pointed out in Ref. [16] that squeezing in the resonant fluorescence is related to quantum fluctuations in the atomic state. However, the relation between quantum fluctuations of the collective atomic state and those of the emitted photon state has yet to be fully explored from the standpoint of the control of few-photon states. The aim of the present paper is to show that we can generate quantum-controlled few-photon states by preparing the atoms in a *squeezed atom state* (SAS), which is a collective state of quantum-mechanically correlated atoms whose quantum fluctuations in population difference or collective dipole are suppressed to below those of the coherent atom state (CAS) [17]. The SAS can be generated via the interaction of atoms with a coherent state of photons in the

cavity having a high quality factor [18]. It will be shown in Sec. V that the SAS can be used as a tunable source of squeezed radiation. This is owing to the fact that quantum fluctuations of the atomic state are rather faithfully transferred to those of the emitted photon state. It will be shown that the number-phase uncertainty relation of photons can be manipulated only if the atoms are in the SAS.

It is well known that the state of a two-level atom can be mapped onto that of a spin 1/2. A collection of  $N$  two-level atoms can be described with a system of spins whose magnitudes are at most  $N/2$ . In particular, if all atoms are in the same pure state, the collective atomic state can be described by a single spin  $N/2$ . The concept of squeezing in the spin or SU(2) algebra [16,19–26] provides a mathematical definition of squeezed states in a system of two-level atoms and in other systems that can be described by the spin algebra. Yurke *et al.* [21] has pointed out that the Mach-Zehnder interferometer is described by spin, and that its phase sensitivity can reach the fundamental limit of  $2/N$  using an  $N$  particle squeezed state. Kitagawa and Ueda [25] showed that such a squeezed state can be realized using the Coulomb interaction between charged particles. Wineland *et al.* [26] applied the SAS to Ramsey spectroscopy and showed that its sensitivity can surpass that of uncorrelated atoms.

This paper is organized as follows. Section II briefly reviews the interaction between two-level atoms and photons in the cavity. Section III defines the SAS in terms of the spin representation of two-level atoms and discusses its physical meaning. Section IV analyzes dynamical processes to generate the SAS. Section V describes how quantum-controlled radiation is generated from squeezed atoms. Section VI discusses possible experimental schemes to implement our theory. Some complicated algebraic manipulations are relegated to the appendices to avoid digressing from the main subjects.

## II. INTERACTION BETWEEN PHOTONS AND TWO-LEVEL ATOMS IN THE LOSSLESS CAVITY

The EM-field operator in a lossless cavity can be written as

$$\hat{\mathbf{E}}(\mathbf{r}) = i \sum_n \sqrt{\frac{\hbar\omega_n}{2\varepsilon_0}} [\mathbf{f}_n(\mathbf{r})\hat{a}_n - \mathbf{f}_n^*(\mathbf{r})\hat{a}_n^\dagger], \quad (1)$$

where  $\hat{a}_n^\dagger$  and  $\hat{a}_n$  are the creation and annihilation operators of the EM field for the  $n$ th mode, and  $\mathbf{f}_n(\mathbf{r})$  is the corresponding orthonormal mode function satisfying  $(\nabla^2 + \omega_n^2/c^2)\mathbf{f}_n = \mathbf{0}$ ,  $\nabla \cdot \mathbf{f}_n(\mathbf{r}) = 0$ , and on the boundary the tangential component is required to vanish:  $\mathbf{f}_{n\parallel}(\mathbf{r}) = \mathbf{0}$ . The Hamiltonian of the EM field in the cavity is given by

$$\hat{H}_F = \sum_n \hbar\omega_n \hat{a}_n^\dagger \hat{a}_n. \quad (2)$$

Here and henceforth, zero-point energies are ignored because they do not affect the following discussions.

Suppose that atoms have the upper energy band  $|e_{j\alpha}\rangle$  and the lower energy band  $|g_{j\beta}\rangle$ , where  $j$  distinguishes atoms, and  $\alpha$  and  $\beta$  denote Zeeman sublevels, if any, of the upper and lower energy bands, respectively. When the sublevels in each band are degenerate, the Hamiltonian of  $N$  identical atoms have the form

$$\hat{H}_A = \sum_{j=1}^N \frac{\hbar\omega_A}{2} \left( \sum_{\alpha} |e_{j\alpha}\rangle \langle e_{j\alpha}| - \sum_{\beta} |g_{j\beta}\rangle \langle g_{j\beta}| \right), \quad (3)$$

where  $\hbar\omega_A$  is the energy separation between the two bands. We consider a situation in which a collection of two-level atoms is placed in the cavity, and interacts with the EM field via the electric-dipole interaction described by

$$\hat{H}_I = - \sum_{j=1}^N \hat{\mathbf{D}}_j \cdot \hat{\mathbf{E}}(\hat{\mathbf{R}}_j), \quad (4)$$

where  $\hat{\mathbf{D}}_j = -e \sum_k (\hat{\mathbf{r}}_{jk} - \hat{\mathbf{R}}_j)$  denotes the electric-dipole operator of the  $j$ th atom, which is the sum of differences between the position of the nucleus  $\hat{\mathbf{R}}_j$  and the positions of the electrons  $\hat{\mathbf{r}}_{jk}$  that belong to the  $j$ th atoms. We neglect the dynamics of the center-of-mass motion of atoms, and replace  $\hat{\mathbf{R}}_j$  with a c-number. Making the rotating-wave approximation in the Hamiltonian (4), we obtain

$$\begin{aligned} \hat{H}_I = & - \sum_{j=1}^N \sum_{\alpha, \beta} \sum_n i \sqrt{\frac{\hbar\omega_n}{2\varepsilon_0}} \\ & \times \left[ \mathbf{f}_n(\mathbf{R}_j) |e_{j\alpha}\rangle \langle e_{j\alpha}| \hat{\mathbf{D}}_j |g_{j\beta}\rangle \langle g_{j\beta}| \hat{a}_n - \text{H.c.} \right], \quad (5) \end{aligned}$$

where H.c. denotes the Hermite conjugate of the preceding term.

We assume that only a single mode of the EM field having energy  $\hbar\omega_F$  and a single state for each atomic energy band  $|e_j\rangle$  and  $|g_j\rangle$  participate in the interaction, and omit the subscripts  $n$ ,  $\alpha$ , and  $\beta$  in the following discussions. The Hamiltonian (5) then reduces to

$$\hat{H}_I = \sum_{j=1}^N \frac{1}{2} \left[ \mathbf{d}_j \cdot \mathcal{E}(\mathbf{R}_j) \hat{a} \hat{s}_{j+} + \mathbf{d}_j^* \cdot \mathcal{E}^*(\mathbf{R}_j) \hat{a}^\dagger \hat{s}_{j-} \right], \quad (6)$$

where  $\mathcal{E}(\mathbf{R}_j) = -i\sqrt{2\hbar\omega/\varepsilon_0} \mathbf{f}(\mathbf{R}_j)$  is the amplitude of the electric field per photon,  $\mathbf{d}_j = \langle e_j | \hat{\mathbf{D}}_j | g_j \rangle$  is the electric-dipole matrix element, and  $\hat{s}_{j+} \equiv |e_j\rangle \langle g_j|$  and  $\hat{s}_{j-} \equiv |g_j\rangle \langle e_j|$  are the raising and lowering operators for the  $j$ th atom. Provided that the dipole moment is the same for all atoms, the subscript  $j$  in  $\mathbf{d}_j$  may be omitted. We define three operators  $\hat{s}_{jx} \equiv (\hat{s}_{j+} + \hat{s}_{j-})/2$ ,  $\hat{s}_{jy} \equiv (\hat{s}_{j+} - \hat{s}_{j-})/2i$ , and  $\hat{s}_{jz} \equiv (|e_j\rangle \langle e_j| - |g_j\rangle \langle g_j|)/2$ , which can be verified to obey the spin commutation relation  $[\hat{s}_{jx}, \hat{s}_{jy}] = i\delta_{jj'} \hat{s}_{jz}$  and its cyclic permutations. The two-level atom can therefore be described by spin 1/2. The subscripts  $x$ ,  $y$ , and  $z$  do not denote spatial directions, but the expectation value of the operator  $\hat{s}_{jz} + \frac{1}{2}$  represents the probability of the  $j$ th atom being found in the excited state, and  $\hat{s}_{jx}$  and  $\hat{s}_{jy}$  indicate the quadrature-phase components of the oscillating dipole. This can be seen by rewriting the dipole operator in the form

$$\begin{aligned} \hat{\mathbf{D}}_j &= \mathbf{d} |e_j\rangle \langle g_j| + \mathbf{d}^* |g_j\rangle \langle e_j| \\ &= \mathbf{d} \hat{s}_{j+} + \mathbf{d}^* \hat{s}_{j-} \\ &= 2 [\text{Re}(\mathbf{d}) \hat{s}_{jx} - \text{Im}(\mathbf{d}) \hat{s}_{jy}]. \quad (7) \end{aligned}$$

The spatial direction of the dipole depends on how we excite atoms. For example, if the electric field at the position of an atom is linearly polarized, the dipole oscillates along the same direction. If the electric field at the position of the atom is circularly polarized, the dipole also rotates in time.

Suppose that all atoms are located in a region small in comparison with the wavelength of the field, but that they are not located too closely together in order to avoid direct interactions between them. The Hamiltonian of the entire system is then given by

$$\hat{H} = \hbar\omega_F \hat{a}^\dagger \hat{a} + \hbar\omega_A \hat{S}_z + \hbar g \left( \hat{a} \hat{S}_+ + \hat{a}^\dagger \hat{S}_- \right), \quad (8)$$

where the coupling constant  $g \equiv \mathcal{E}(\mathbf{R}_j) \cdot \mathbf{d}/(2\hbar)$  is taken to be real without loss of generality, and the collective spin operators are defined by

$$\hat{S}_\mu \equiv \sum_j \hat{s}_{j\mu} \quad (\mu = x, y, z), \quad (9)$$

and  $\hat{S}_\pm \equiv \hat{S}_x \pm i\hat{S}_y$ . It is easy to show that these collective operators follow the commutation relation of spin,  $[\hat{S}_x, \hat{S}_y] = i\hat{S}_z$ , and its cyclic permutations. The Hamiltonian (8) is referred to as the Jaynes-Cummings (JC) Hamiltonian [27].

It is worth pointing out that one can introduce the collective spin operators when the magnitudes of  $\mathcal{E}(\mathbf{R}_j) \cdot \mathbf{d}_j$  in the Hamiltonian (6) are the same for all the atoms but their phases are different due, e.g., to different spatial locations of the atoms. The collective spin operators in this case may be defined as

$$\hat{S}'_{\pm} \equiv \sum_j e^{\pm i\phi_j} \hat{s}_{j\pm}, \quad \hat{S}_z \equiv \sum_j \hat{s}_{jz}, \quad (10)$$

where  $\phi_j$  is the phase of  $\mathbf{E}(\mathbf{R}_j) \cdot \mathbf{d}_j$ . For example, when atoms are located in a one-dimensional standing wave at every half wavelength, we have  $\phi_j = j\pi$ . The operators (10) also satisfy the spin commutation relations and the Hamiltonian of the system is given by Eq. (8) in which  $\hat{S}_{\pm}$  is replaced by  $\hat{S}'_{\pm}$ . Even if the spin state described by the operators (10) and that described by the operators (9) are the same, the corresponding states of atoms are different. When atoms are located in the same place the dipoles oscillate in phase. When they are located at every half wavelength, the neighboring dipoles oscillate out of phase. Nevertheless, the photon states generated by these atoms via the JC Hamiltonian (8) are the same.

When we move to the rotating frame for both the photon field and the atoms via a unitary transformation  $\hat{U}_0(t) = e^{i(\omega_F \hat{a}^\dagger \hat{a} + \omega_A \hat{S}_z)t}$ , the Hamiltonian (8) is transformed to

$$\hat{U}_0 \hat{H} \hat{U}_0^\dagger + i\hbar \frac{\partial \hat{U}_0}{\partial t} \hat{U}_0^\dagger = g\hbar(\hat{a} \hat{S}_+ e^{-i\delta t} + \hat{a}^\dagger \hat{S}_- e^{i\delta t}), \quad (11)$$

where  $\delta = \omega_F - \omega_A$  denotes the detuning between the atoms and the field. When  $\delta$  is zero, Eq. (11) becomes

$$\hat{H}^{\text{rot}} = \hbar g (\hat{a} \hat{S}_+ + \hat{a}^\dagger \hat{S}_-). \quad (12)$$

This commutes with the rotation operator,

$$\hat{U}(\varphi) \equiv e^{-i\varphi(\hat{a}^\dagger \hat{a} + \hat{S}_z)}, \quad (13)$$

and is therefore invariant under rotation. This rotational invariance allows us to choose a convenient frame of reference without loss of generality. For instance, when initially the EM field is in the coherent state  $|\alpha\rangle$  and the atoms are in the fully excited state  $|S, M=S\rangle$ , we can arbitrarily choose the phase of the initial coherent state without loss of generality. Time development from the other initial state  $|\alpha e^{-i\varphi}\rangle|S, M=S\rangle$  can be obtained by a mere rotation  $\hat{U}(\varphi)$ .

### III. SQUEEZING IN COLLECTIVE TWO-LEVEL ATOMS

As shown in the preceding section, a collection of two-level atoms can be described by collective spin operators (9). An eigenvalue of the Casimir operator  $\hat{\mathbf{S}}^2 = \hat{S}_x^2 + \hat{S}_y^2 + \hat{S}_z^2$  is given by  $S(S+1)$ , where the total spin  $S$  can take on values,  $S = \frac{N}{2}, \frac{N}{2} - 1, \dots, 0$  (or  $1/2$ ) when the number of atoms  $N$  is even (or odd). For each total spin  $S$  there are  $N!(2S+1)/[(\frac{1}{2}N+S+1)!(\frac{1}{2}N-S)!]$  different subspaces. Generally speaking, a state of  $N$  two-level atoms can be described by a mixture of these subspaces.

Because the JC Hamiltonian (8) is described by the collective spin operators which never mix the subspaces having different total spins, we will restrict our discussions to a single subspace having the maximal total spin  $N/2$ . This state can be most easily accessed from the state in which all the atoms are either in the ground state or in the excited state. It is interesting to note that the subspaces having the same total spin behave exactly the same within the JC model if the numbers of atoms are different. For example, the state of two atoms having the total spin 1 and that of 100 atoms having the same total spin 1 obey the same JC Hamiltonian. No single-mode photon field distinguishes between these atomic states through the JC interaction.

A state of the single-mode photon field is defined as squeezed if, for a nonzero range of parameter  $\phi$ ,  $\langle(\Delta\hat{a}_\phi)^2\rangle$  is smaller than that of the coherent state — the standard quantum limit (SQL) — of  $1/4$ , where  $\hat{a}_\phi$  is defined as

$$\hat{a}_\phi \equiv \frac{1}{2}(\hat{a}e^{-i\phi} + \hat{a}^\dagger e^{i\phi}). \quad (14)$$

The canonical commutation relation is given by  $[\hat{a}_\phi, \hat{a}_{\phi+\pi/2}^\dagger] = i/2$ , and the conventional in-phase and out-of-phase components  $\hat{a}_1$  and  $\hat{a}_2$  can be expressed as  $\hat{a}_1 = \hat{a}_{\phi=0}$  and  $\hat{a}_2 = \hat{a}_{\phi=\pi/2}$ , respectively. From the commutation relation we have

$$\langle(\Delta\hat{a}_\phi)^2\rangle\langle(\Delta\hat{a}_{\phi+\pi/2})^2\rangle \geq \frac{1}{16}. \quad (15)$$

The coherent state has the variance of  $\langle(\Delta\hat{a}_\phi)^2\rangle = 1/4$  for any  $\phi$  and satisfies the equality in Eq. (15). The profile of quantum fluctuations of a photon state described by a density operator  $\hat{\rho}_F$  can be visualized with the quasi-probability distribution

$$Q(\alpha) \equiv \frac{1}{\pi} \langle \alpha | \hat{\rho}_F | \alpha \rangle, \quad (16)$$

where  $|\alpha\rangle$  is the coherent state with amplitude  $\alpha$ . The quasi-probability distribution of the coherent state is isotropic and that of the quadrature-amplitude squeezed state is elliptic.

The coherent state of a spin- $S$  system is defined by

$$\begin{aligned} |\theta, \phi\rangle &\equiv \exp[i\theta(\hat{S}_x \sin \phi - \hat{S}_y \cos \phi)] |S, M=S\rangle \\ &= \sum_{M=-S}^S \binom{2S}{S+M}^{\frac{1}{2}} e^{i(S-M)\phi} \\ &\quad \times \left(\sin \frac{\theta}{2}\right)^{S-M} \left(\cos \frac{\theta}{2}\right)^{S+M} |S, M\rangle, \end{aligned} \quad (17)$$

which is referred to as the coherent spin state (CSS) or the Bloch state [17]. The mean spin vector of the CSS  $|\theta, \phi\rangle$  points in the direction  $\mathbf{n} = \langle\hat{\mathbf{S}}\rangle/|\langle\hat{\mathbf{S}}\rangle| = (\sin \theta \cos \phi, \sin \theta \sin \phi, \cos \theta)$ , where  $|\langle\hat{\mathbf{S}}\rangle| = (\langle\hat{S}_x\rangle^2 + \langle\hat{S}_y\rangle^2 + \langle\hat{S}_z\rangle^2)^{1/2}$ . Denoting  $\mathbf{m}$  as the unit vector that

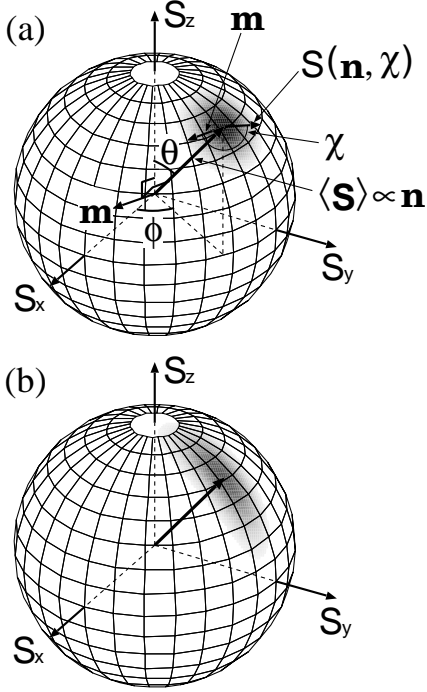


FIG. 1. The quasi-probability distributions of (a) the coherent spin state and (b) the squeezed spin state. The unit vector  $\mathbf{n}$  points in the direction of the mean spin vector, and the unit vector  $\mathbf{m}$  is normal to both  $\mathbf{n}$  and the  $S_z$  direction. The spin component  $S(\mathbf{n}, \chi)$  is normal to the mean spin vector, and the angle  $\chi$  is measured from  $\mathbf{m}$ .

is normal to both  $\mathbf{n}$  and the unit vector of the  $z$  direction  $\mathbf{e}_z$ , namely,  $\mathbf{m} = \mathbf{n} \times \mathbf{e}_z / |\mathbf{n} \times \mathbf{e}_z| = (\sin \phi, -\cos \phi, 0)$ , we may express  $|\theta, \phi\rangle$  as

$$|\theta, \phi\rangle = \exp[i\theta \mathbf{m} \cdot \hat{\mathbf{S}}] |S, M = S\rangle. \quad (18)$$

When a system of two-level atoms is described by Eq. (17) in the spin representation, we will say that the atoms are in a coherent atom state (CAS). The component of  $\hat{\mathbf{S}}$  normal to the mean spin vector is given by

$$\hat{S}(\mathbf{n}, \chi) = \exp(-i\chi \hat{\mathbf{S}} \cdot \mathbf{n}) (\hat{\mathbf{S}} \cdot \mathbf{m}) \exp(i\chi \hat{\mathbf{S}} \cdot \mathbf{n}), \quad (19)$$

where  $\chi$  denotes the angle defined on the plane normal to the mean spin vector (see Fig. 1(a)). The commutation relation between the two quadrature components is given by

$$[\hat{S}(\mathbf{n}, \chi), \hat{S}(\mathbf{n}, \chi + \pi/2)] = i\hat{\mathbf{S}} \cdot \mathbf{n}, \quad (20)$$

and the corresponding uncertainty relation is given by

$$\langle [\Delta \hat{S}(\mathbf{n}, \chi)]^2 \rangle \langle [\Delta \hat{S}(\mathbf{n}, \chi + \pi/2)]^2 \rangle \geq \frac{|\langle \hat{\mathbf{S}} \rangle|^2}{4}. \quad (21)$$

The CSS satisfies the equality in the uncertainty relation (21), and  $\langle [\Delta \hat{S}(\mathbf{n}, \chi)]^2 \rangle = S/2$  for any  $\chi$ . The CSS therefore has an isotropic fluctuation normal to the mean spin vector as shown in Fig. 1(a), where the spin state is visualized with the quasi-probability distribution of spin defined by

$$Q_s(\theta, \phi) = \frac{2S+1}{4\pi} \langle \theta, \phi | \hat{\rho}_A | \theta, \phi \rangle, \quad (22)$$

where  $\hat{\rho}_A$  is the density operator of a collective atomic state. Analogous to the case of photons, a spin state is defined as squeezed if the following inequality holds for a certain  $\chi$ :

$$\langle [\Delta \hat{S}(\mathbf{n}, \chi)]^2 \rangle < \frac{|\langle \hat{\mathbf{S}} \rangle|}{2}. \quad (23)$$

That is, the squeezed spin state (SSS) is a state whose fluctuation of one component normal to the mean spin vector is less than half of the length of the mean spin vector. When the condition (23) is satisfied, the variance of the quadrature component  $\langle [\Delta \hat{S}(\mathbf{n}, \chi + \pi/2)]^2 \rangle$  must be larger than  $|\langle \hat{\mathbf{S}} \rangle|/2$  in order to obey the uncertainty relation (21), and hence the fluctuation profile on the spin sphere becomes elliptic, as shown in Fig. 1(b).

Squeezing in spin or angular momentum has been discussed by many authors [16,19–26]. However, the definitions of the SSS in Refs. [16,19,20,22–24] depend on the specific spin coordinates and are therefore not invariant under rotation in the spin space. It was pointed out in Ref. [25] that the direction of the mean spin vector  $\mathbf{n}$  should be taken into account to define the SSS in a rotation-invariant manner as in Eq. (23).

Mathematically, SSS satisfying the condition (23) can be generated by unitary transformations from the CSS. The unitary transformations have the forms  $\exp(-i\xi \hat{S}_z^2) |\theta = \pi/2, \phi\rangle$  and  $\exp[-i\eta(\hat{S}_+^2 - \hat{S}_-^2)] |\theta = 0, \phi\rangle$ , where  $\xi$  and  $\eta$  denote the parameters that characterize the degree of one-axis twisting and that of two-axis counter-twisting, respectively [25].

Let us return to the spin representation of two-level atoms. We define the squeezed atom state (SAS) as a state of two-level atoms that are in the SSS in the spin representation. We note that quantum-mechanical correlations between atoms must be established for the atoms to be in an SAS. The state in which all atoms are in their ground state is in a CAS  $|\theta = \pi, \phi\rangle$  in the spin representation, and not in an SAS. If they are irradiated by a  $\pi/2$  pulse, the spin state becomes  $|\theta = \pi/2, \phi\rangle$ , which is also not squeezed, because atoms are described by the same state and are not quantum-mechanically correlated with each other. We also note that a single atom cannot be squeezed, since  $\langle [\Delta \hat{S}(\mathbf{n}, \chi)]^2 \rangle$  is always  $1/4 (= S/2)$  for spin  $1/2$ . In other words, the single atom cannot

be squeezed because it has no partner with which to be quantum-mechanically correlated.

According to the definitions of the collective spin operators (9),  $\hat{S}_z$  represents the population difference of two-level atoms, and  $\hat{S}_x$  and  $\hat{S}_y$  represent quadrature-phase components of the electric dipole. Squeezing of the  $\hat{S}_z$  component thus means reduced fluctuations in the population difference at the expense of the enhanced dipole fluctuation, while squeezing of  $\hat{S}_x$ ,  $\hat{S}_y$ , or their arbitrary linear combination

$$\hat{S}_\phi \equiv \frac{1}{2} (\hat{S}_+ e^{-i\phi} + \hat{S}_- e^{i\phi}). \quad (24)$$

means reduced dipole fluctuations at the expense of the enhanced fluctuations in the population difference.

To measure the  $\hat{S}_z$  component, one can use an ionization detector which counts the number of atoms in the excited state. If such measurement is carried out repeatedly, with the atoms prepared in the same state for every measurement, the variance of the population difference  $\langle (\Delta \hat{S}_z)^2 \rangle$  is obtained. Variances of the other spin components can be measured by rotating the spin state so that they become the  $\hat{S}_z$  component. The rotation in the spin space can be realized by irradiation of maser or laser with classical intensity to the atoms. The frequency of the maser or laser is assumed to be resonant with the transition frequency of the atom. The Hamiltonian describing the irradiation process of the classical field is obtained by replacing the operator  $\hat{a}$  with a c-number  $\alpha$  in the JC Hamiltonian (12),

$$\begin{aligned} \hat{H}_{\text{cl}} &= \hbar g (\alpha \hat{S}_+ + \alpha^* \hat{S}_-) \\ &= 2\hbar g |\alpha| (\hat{S}_x \cos \phi_c - \hat{S}_y \sin \phi_c), \end{aligned} \quad (25)$$

where  $\phi_c = \arg \alpha$  is the phase of the classical field. The Hamiltonian (25) rotates the spin vector about the axis  $\hat{S}_{\phi_c}$  through angle  $2g|\alpha|T_i$ , where  $T_i$  is the irradiation time. For example, the  $\hat{S}_x$  component can be measured by counting the population difference with the ionization detector after irradiation of the classical field corresponding to the operation  $\exp(-i\frac{\pi}{2}\hat{S}_y)$ . In this operation the collective dipole of the atoms  $\hat{S}_x$  is converted to the population difference  $\hat{S}_z$ .

#### IV. PREPARATION OF SQUEEZED ATOM STATES

Several schemes for generating the SAS have been proposed. Barnett and Dupertuis [23] considered the interaction of the antisymmetric collective dipole with the coherent EM field. Agarwal and Puri [24] examined the steady state of atoms interacting with broadband squeezed radiation. Although a coordinate-dependent definition of spin squeezing  $\langle (\Delta \hat{S}_{x(y)})^2 \rangle < |\langle \hat{S}_z \rangle|/2$  is used in Refs. [23] and [24], the states constructed there

also satisfy the coordinate-independent condition (23). Wineland *et al.* [26] considered the stimulated Raman coupling between kinetic motion of atoms in an ion trap and internal levels of atoms, and showed that by initially squeezing the kinetic motion one can generate the SAS of the internal state via the JC interaction. They also showed that the coherent state of the kinetic motion can generate the SAS via the parametric-type interaction. Kuzmich *et al.* [28] considered V-type three-level atoms driven by squeezed light that leads to the SAS.

In the present paper we follow the scheme proposed in Ref. [18], namely the interaction between the atoms and the coherent state of photons in a high-Q cavity. The higher-order interaction between atoms and photons establishes the quantum correlation between the atoms, thereby reducing the dipole fluctuation. This scheme is simple in that no special field state, other than the coherent state, is required.

#### A. Analysis for the case of two atoms

The JC model can be solved exactly for up to three atoms, and in the zero-detuning case for up to eight atoms. We will henceforth assume zero detuning  $\delta = 0$ , and employ the Hamiltonian (12). By exactly solving the dynamical evolution for two atoms, we discuss the properties of this system.

We consider the case in which both atoms are initially in the excited state  $|S = 1, M = 1\rangle \equiv |1, 1\rangle_A$  and photons are in an arbitrary superposition state  $\sum_n c_n |n\rangle_F$ , where  $|n\rangle_F$  is the photon-number state. The time development is calculated to be [18]

$$\begin{aligned} |\psi(t)\rangle &= e^{-\frac{i}{\hbar} \hat{H}^{\text{rot}} t} |n\rangle_F |1, 1\rangle_A \\ &= \sum_{n=0}^{\infty} c_n e^{-i(n+1)\omega_F t} [p_n(t) |1, 1\rangle_A |n\rangle_F \\ &\quad + q_n(t) |1, 0\rangle_A |n+1\rangle_F + r_n(t) |1, -1\rangle_A |n+2\rangle_F], \end{aligned} \quad (26)$$

where

$$p_n(t) = \frac{(n+1) \cos \sqrt{2(2n+3)gt} + n+2}{2n+3}, \quad (27a)$$

$$q_n(t) = -i \sqrt{\frac{n+1}{2n+3}} \sin \sqrt{2(2n+3)gt}, \quad (27b)$$

$$r_n(t) = \frac{\sqrt{(n+1)(n+2)}}{2n+3} (\cos \sqrt{2(2n+3)gt} - 1). \quad (27c)$$

One can calculate any physical quantities from this solution.

Let us first consider the photon-number state  $|n\rangle_F$  as the initial state. In this case the initial state  $|n\rangle_F |1, 1\rangle_A$  is invariant with respect to rotation (13), and consequently  $\langle \hat{S}_x \rangle = \langle \hat{S}_y \rangle = 0$ , which remains true at later times. The

variances of the components normal to the mean spin vector are calculated to be

$$\begin{aligned}\langle(\Delta\hat{S}_x)^2\rangle &= \langle(\Delta\hat{S}_y)^2\rangle \\ &= \frac{1}{2} \left( 1 + \frac{n+1}{2n+3} \sin^2 \sqrt{2(2n+3)gt} \right),\end{aligned}\quad (28)$$

which is always greater than  $S/2 = 1/2$ , and hence the spin state can never be squeezed. Generally, when the initial state is invariant with respect to the rotation  $\hat{U}(\varphi)$ , the atoms can never be squeezed for any number of atoms.

When the photon field is initially in the coherent state  $|\alpha\rangle$ , the coefficients are given by  $c_n = e^{-|\alpha|^2/2} \alpha^n / \sqrt{n!}$ . The amplitude  $\alpha$  can be taken to be real without loss of generality, and in this case  $\langle\hat{a}_2\rangle$  and  $\langle\hat{S}_x\rangle$  vanish at any time (see appendix A). Therefore the  $S_x$  direction is always normal to the mean spin vector. The variance of  $\hat{S}_x$  is calculated to be

$$\begin{aligned}\langle(\Delta\hat{S}_x)^2\rangle &= e^{-|\alpha|^2} \sum_{n=2}^{\infty} \frac{\alpha^{2n-2}}{\sqrt{n!(n-2)!}} p_n(t) r_{n-2}(t) \\ &\quad + \frac{1}{2} e^{-|\alpha|^2} \sum_{n=0}^{\infty} \frac{\alpha^{2n}}{n!} [p_n(t)^2 + 2q_n(t)^2 + r_n(t)^2].\end{aligned}\quad (29)$$

When  $\alpha \gg 1$ , the photon-number distribution has a narrow peak relative to the mean photon number  $\bar{n}$ , and one can expand (29) with respect to  $n - \bar{n}$ . Replacing the summations with the integrals we obtain, for  $gt \lesssim 1/\sqrt{\bar{n}}$ ,

$$\langle(\Delta\hat{S}_x)^2\rangle \simeq \frac{1}{2} - \frac{1}{2\bar{n}} \sin^4 \sqrt{\bar{n}}gt + \frac{gt}{2\sqrt{\bar{n}}} \sin 2\sqrt{\bar{n}}gt. \quad (30)$$

Similarly,  $\langle\hat{S}_y\rangle$  and  $\langle\hat{S}_z\rangle$  are approximated to be

$$\begin{aligned}\langle\hat{S}_y\rangle &\simeq -e^{-(gt)^2/2} \sin 2\sqrt{\bar{n}}gt - \frac{gt}{\sqrt{\bar{n}}} \left( \frac{3}{4} - \frac{5}{2} \sin^2 \sqrt{\bar{n}}gt \right) \\ &\quad + \frac{1}{8\bar{n}} (\sin 2\sqrt{\bar{n}}gt + \sin 4\sqrt{\bar{n}}gt),\end{aligned}\quad (31a)$$

$$\begin{aligned}\langle\hat{S}_z\rangle &\simeq e^{-(gt)^2/2} \cos 2\sqrt{\bar{n}}gt - \frac{5gt}{4\sqrt{\bar{n}}} \sin 2\sqrt{\bar{n}}gt \\ &\quad + \frac{1}{4\bar{n}} \sin^2 2\sqrt{\bar{n}}gt.\end{aligned}\quad (31b)$$

Therefore, if the squeezing factor defined by

$$\begin{aligned}\frac{\langle(\Delta\hat{S}_x)^2\rangle}{|\langle\hat{\mathbf{S}}\rangle|/2} &\simeq e^{\frac{(gt)^2}{2}} - \frac{1}{\bar{n}} \sin^2 \sqrt{\bar{n}}gt + \frac{3}{8\bar{n}} \sin^2 2\sqrt{\bar{n}}gt \\ &\quad + \frac{3gt}{2\sqrt{\bar{n}}} \sin 2\sqrt{\bar{n}}gt\end{aligned}\quad (32)$$

is less than one, the condition for the SAS (23) is fulfilled. Figure 2 compares the time evolution of the approximate formula (32) (dashed curve) with the exact one which is numerically calculated from (26) (solid curve)

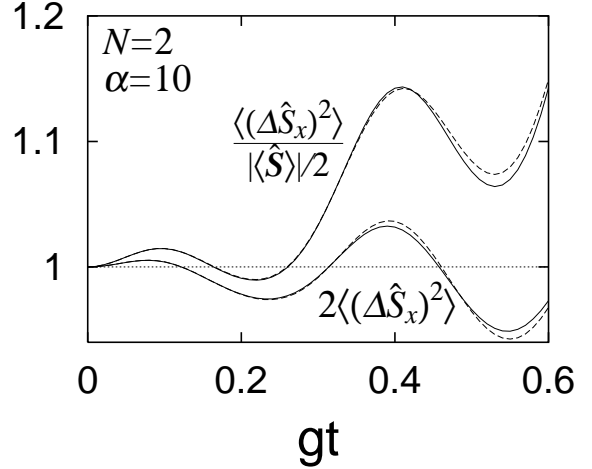


FIG. 2. Time evolutions of the normalized variance  $2\langle(\Delta\hat{S}_x)^2\rangle$  and the squeezing factor  $2\langle(\Delta\hat{S}_x)^2\rangle/|\langle\hat{\mathbf{S}}\rangle|$  for two atoms. The two atoms are initially excited, and the EM field is initially in the coherent state with amplitude  $\alpha = 10$ . The solid curves show the numerical results, and the dashed ones show approximate solutions (30) and (32).

for two atoms and for  $\bar{n} = \alpha^2 = 100$ . The parameter  $gt$  in Fig. 2 and all the quantities appearing in the figures presented henceforth are dimensionless. We find that both curves are in excellent agreement and the SAS is attained around  $gt = 0.2$ . The variance of another component that is normal to both the mean spin vector and the  $S_x$  direction never reduces to below  $1/2$ . It can be shown numerically that the SAS never occurs after the first minimum around  $gt = 0.2$ . Although in Fig. 2 the second minimum of the variance  $\langle(\Delta\hat{S}_x)^2\rangle$  goes below the first minimum, the squeezing factor does not go below the first minimum because the length of the spin vector also decreases.

Equation (32) shows that squeezing vanishes when the intensity of the coherent state is sufficiently large,  $\bar{n} \gg 1$ , which is due to the fact that the classical field merely rotates the spin vector. The photon-number state cannot produce the SAS, as mentioned above. We thus find that both wave and particle aspects of photons are necessary for atoms to be squeezed.

## B. Analytic approach for the case of a large number of atoms

We provide here approximate analytic expressions for the case of a large number of atoms. These are derived by neglecting the terms of order  $1/N$  relative to the dominant terms in the equations of motion, which are therefore very accurate when the number of atoms  $N$  is very large.

The initial state is assumed to be the totally excited state of the atoms  $|S, M = S\rangle$  and the coherent state of the field  $|\alpha\rangle$ , where  $\alpha$  is assumed to be real and hence  $\langle\hat{S}_x\rangle = \langle\hat{a}_2\rangle = 0$ . The other averages obey the equations of motion (see appendix B for derivations),

$$\frac{d\langle\hat{S}_y\rangle}{dt} \simeq -2g\langle\hat{a}_1\rangle\langle\hat{S}_z\rangle, \quad (33a)$$

$$\frac{d\langle\hat{S}_z\rangle}{dt} \simeq 2g\langle\hat{a}_1\rangle\langle\hat{S}_y\rangle, \quad (33b)$$

$$\frac{d\langle\hat{a}_1\rangle}{dt} \simeq -g\langle\hat{S}_y\rangle, \quad (33c)$$

which become those of a pendulum, if we set

$$\langle\hat{S}_y\rangle = \frac{N}{2} \sin \theta, \quad (34a)$$

$$\langle\hat{S}_z\rangle = \frac{N}{2} \cos \theta, \quad (34b)$$

$$\langle\hat{a}_1\rangle = -\frac{1}{2g} \frac{d\theta}{dt}. \quad (34c)$$

The solutions of Eqs. (33a) can be expressed in terms of Jacobi's elliptic functions [29]. Solving the equations of motion for fluctuations, we obtain

$$\langle(\Delta\hat{a}_2)^2\rangle = \frac{1}{4\text{dn}^2(u|m)} [1 + mE^2(u|m)], \quad (35a)$$

$$\begin{aligned} \langle(\Delta\hat{S}_x)^2\rangle = \frac{N}{4} \Bigg\{ & m \frac{\text{sn}^2(u|m)\text{cn}^2(u|m)}{\text{dn}^4(u|m)} \\ & + \left[ m \frac{\text{sn}(u|m)\text{cn}(u|m)}{\text{dn}^2(u|m)} E(u|m) \right. \\ & \left. + \text{dn}(u|m) \right]^2 \Bigg\}, \end{aligned} \quad (35b)$$

where  $u \equiv gt\sqrt{N + \alpha^2}$  and  $m \equiv N/(N + \alpha^2)$ . Jacobi's elliptic functions [29] are defined by  $\text{sn}(u|m) = \sin \varphi$ ,  $\text{cn}(u|m) = \cos \varphi$ ,  $\text{dn}(u|m) = \sqrt{1 - m \sin^2 \varphi}$ , where  $u$  and  $\varphi$  are related by

$$u = \int_0^\varphi \frac{d\theta}{\sqrt{1 - m \sin^2 \theta}}. \quad (36)$$

The elliptic integral of the second kind is given by  $E(u|m) = \int_0^u \text{dn}^2(u'|m) du'$ .

Figure 3 compares the analytic solutions (35) (dashed curves) with the numerically exact ones (solid curves) for 100 atoms and  $\alpha = 10$ . We find that the analytic curves are in excellent agreement with the numerical ones. The analytic curves, however, begin to deviate from the numerical ones at around  $gt \simeq 0.3$ . This is because the differential equations (B4) and (B9) include errors of order  $1/N$  relative to the dominant terms, which accumulate to produce errors in the solutions of order  $e^{gt\sqrt{N}}/N$ , which becomes of order unity around  $gt \simeq 0.3$ .

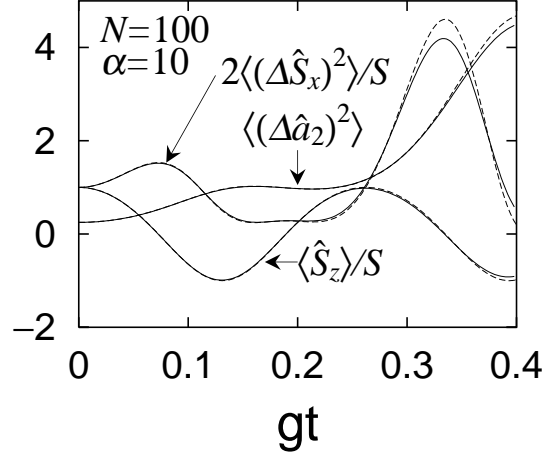


FIG. 3. Time evolutions of  $\langle\hat{S}_z\rangle/S$ ,  $2\langle(\Delta\hat{S}_x)^2\rangle/S$  and  $\langle(\Delta\hat{a}_2)^2\rangle$  for 100 atoms ( $S = 50$ ). All the atoms are initially excited, and the EM field is initially in the coherent state with amplitude  $\alpha = 10$ . The solid curves show the numerical results, and the dashed ones show approximate solutions (35) and (B7b).

The analogy to the pendulum gives us a qualitative and simple account of the squeezing mechanism. When the pendulum points in the direction  $(\sin \theta \cos \phi, \sin \theta \sin \phi, \cos \theta)$ , it undergoes the force toward the direction  $(\cos \theta \cos \phi, \cos \theta \sin \phi, -\sin \theta)$ . In the present case, where  $\alpha$  is taken to be real, the pendulum begins to fall toward the negative  $S_y$  axis and rotates on the  $S_y$ - $S_z$  plane. Suppose that the pendulum has a deviation from the  $S_y$ - $S_z$  plane ( $\phi = -\frac{\pi}{2} + \delta\phi$ ), the direction of the force is  $(\cos \theta \delta\phi, 0, -\sin \theta)$ . This force increases the deviation when  $\cos \theta > 0$ , and decreases it when  $\cos \theta < 0$ . In fact, in Fig. 3,  $\langle(\Delta\hat{S}_x)^2\rangle$  increases when  $\langle\hat{S}_z\rangle > 0$ , and decreases when  $\langle\hat{S}_z\rangle < 0$ .

### C. Numerical analysis

When the number of atoms is intermediate, analytic solutions are unavailable, so we study the dynamical evolution of the system by numerically diagonalizing the Hamiltonian (12). The amount of computation increases with increasing the number of atoms  $N$  roughly as  $N^3$ . The initial state is assumed to be the totally excited state of the atoms  $|S, M = S\rangle$  and the coherent state of the photon field  $|\alpha\rangle$ , where  $\alpha$  is again taken to be real.

Figure 4 shows time evolutions of statistical properties of atoms and photons. The number of atoms is 10, and the amplitude of the initial coherent state is chosen to be  $\alpha = 3.3$  to obtain the maximal squeezing of the atoms. The  $S_x$  component is always normal to the



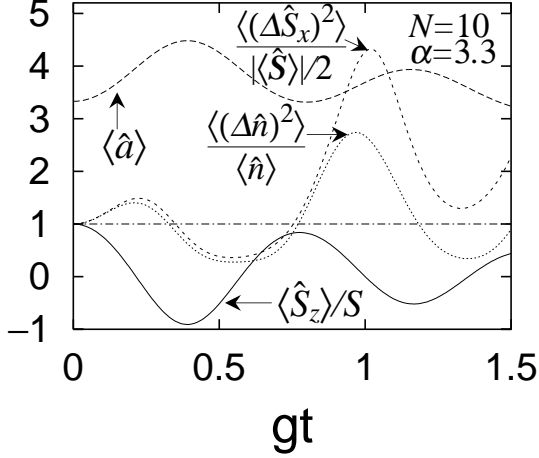


FIG. 4. Time evolutions of  $\langle \hat{S}_z \rangle / S$ ,  $2\langle (\Delta \hat{S}_x)^2 \rangle / |\langle \hat{\mathbf{S}} \rangle|$ ,  $\langle \hat{a} \rangle$  and  $\langle (\Delta \hat{n})^2 \rangle / \langle \hat{n} \rangle$  for 10 atoms ( $S = 5$ ). All the atoms are initially excited, and the EM field is initially in the coherent state with amplitude  $\alpha = 3.3$ .

mean spin vector, since  $\langle \hat{S}_x \rangle = 0$ . In Fig. 4, the squeezing factor  $2\langle (\Delta \hat{S}_x)^2 \rangle / |\langle \hat{\mathbf{S}} \rangle|$  becomes less than one, which indicates that the SAS is obtained. The maximum degree of squeezing is attained in the first minimum. It is found from the long-term behavior that the squeezing never occurs at a later time. The fluctuation of the other component that is normal to both the  $S_x$  direction and the mean spin vector never fulfills the squeezing condition (23). Since the mean spin vector rotates in the  $S_y$ - $S_z$  plane,  $\langle \hat{S}_z \rangle$  oscillates with the amplitude of  $|\langle \hat{\mathbf{S}} \rangle|$ . The amplitude of the photon field also oscillates with the same period but out of phase because of the energy exchange between the atoms and the photon field. The variance  $\langle (\Delta \hat{S}_x)^2 \rangle$  increases when  $\langle \hat{S}_z \rangle > 0$ , and decreases when  $\langle \hat{S}_z \rangle < 0$ , as discussed in the previous subsection. The Fano factor  $\langle (\Delta \hat{n})^2 \rangle / \langle \hat{n} \rangle$  of the photon field also goes below the SQL, and its behavior is very similar to that of  $\langle (\Delta \hat{S}_x)^2 \rangle$ . The long-term behavior of this system is shown in Fig. 5. The collapse and revival phenomena occur in the population difference and in the Fano factor as in the case of a single atom [30]. The revival peak of the Fano factor splits and there is a small revival before the main revival. The variance  $\langle (\Delta \hat{S}_x)^2 \rangle$ , on the other hand, oscillates with the same period as the revivals, and the initially regular oscillations gradually change to random fluctuations around some value.

The degree of squeezing of the SAS depends on the number of atoms  $N$ , and for each  $N$  the maximum degree of squeezing is attained at a particular amplitude  $\alpha$  of the initial coherent state. Figure 6 shows the minimum squeezing factor  $2\langle (\Delta \hat{S}_x)^2 \rangle / |\langle \hat{\mathbf{S}} \rangle|$  for each number of atoms and the amplitude of the initial coherent state

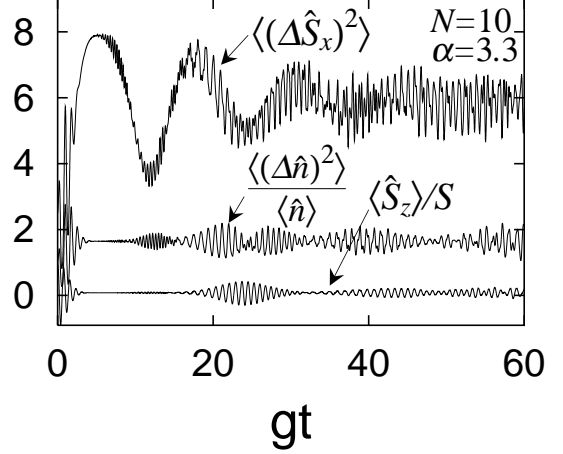


FIG. 5. Long-term behaviors of  $\langle \hat{S}_z \rangle / S$ ,  $\langle (\Delta \hat{S}_x)^2 \rangle$  and  $\langle (\Delta \hat{n})^2 \rangle / \langle \hat{n} \rangle$  for 10 atoms. All the atoms are initially excited, and the photon field is initially in the coherent state with amplitude  $\alpha = 3.3$ .

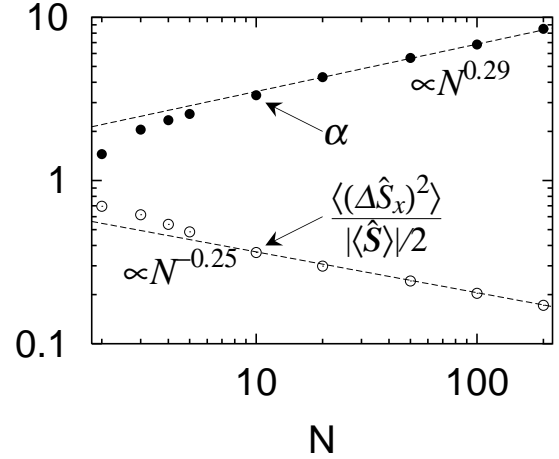


FIG. 6. Minimum values of the squeezing factors  $2\langle (\Delta \hat{S}_x)^2 \rangle / |\langle \hat{\mathbf{S}} \rangle|$  obtained by the interaction of atoms with the coherent states of photons as a function of the number of atoms  $N$ . For each  $N$  the amplitude of the coherent state  $\alpha$  is chosen to give the best squeezing factor. The squeezing factor tends to scale as  $N^{-0.25}$  for large  $N$  and the optimal amplitude  $\alpha$  as  $N^{0.29}$ .

that gives this factor. We find that the higher degree of squeezing can be obtained for the larger number of atoms. The squeezing factor tends to behave as  $N^{-0.25}$  when  $N$  is more than about ten, and the optimal amplitude  $\alpha$  behaves as  $N^{0.29}$ .

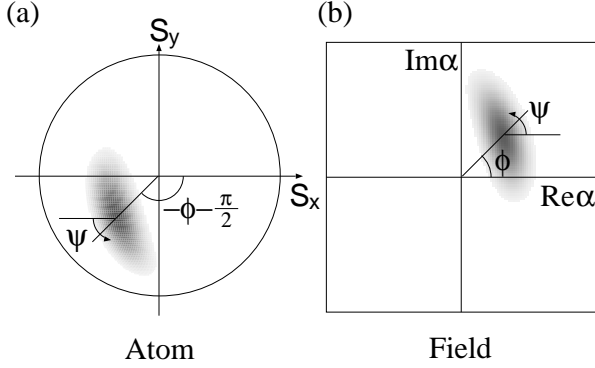


FIG. 7. The relation between (a) the quasi-probability distribution of the prepared atoms (22) and (b) that of the emitted photon field (16). The angle  $\phi$  (or  $-\phi - \pi/2$ ) represents the direction of the mean amplitude of the photon field (or the mean spin vector), and  $\psi$  represents the direction of the fluctuations of the spin and the photon field. The  $S_z$  component of the mean spin vector is negative.

## V. QUANTUM-CONTROLLED RADIATION FROM SQUEEZED ATOMS

It is natural to expect that the atoms whose collective dipole or population difference is squeezed can radiate the photon field having nonclassical properties. We will show that this is indeed the case, and that quantum fluctuations of the photon field can be controlled by manipulating the SAS, which is done by applying a classical field to the atoms.

### A. Radiation from squeezed atoms

The Heisenberg equations of motion for  $\hat{a}_\phi$  and  $\hat{S}_{-\phi-\pi/2}$  are written as

$$\dot{\hat{a}}_\phi = \frac{i}{\hbar} [\hat{H}^{\text{rot}}, \hat{a}_\phi] = g \hat{S}_{-\phi-\pi/2}, \quad (37a)$$

$$\dot{\hat{S}}_{-\phi-\pi/2} = \frac{i}{\hbar} [\hat{H}^{\text{rot}}, \hat{S}_{-\phi-\pi/2}] = 2g \hat{a}_\phi \hat{S}_z. \quad (37b)$$

Equation (37a) indicates that the phase of the photon field is connected with the direction of the spin vector. When the spin vector is tilted toward the direction of  $-\phi - \pi/2$ , the field is initially amplified toward the direction of  $\phi$ , as illustrated in Fig. 7. The equations of motion for various fluctuations are given by

$$\frac{d}{dt} \langle (\Delta \hat{a}_\psi)^2 \rangle = 2g \langle (\Delta \hat{a}_\psi) (\Delta \hat{S}_{-\psi-\pi/2}) \rangle, \quad (38a)$$

$$\frac{d}{dt} \langle (\Delta \hat{a}_\psi) (\Delta \hat{S}_{-\psi-\pi/2}) \rangle = g \left[ \langle (\Delta \hat{S}_{-\psi-\pi/2})^2 \rangle \right.$$

$$\left. + 2 \langle (\Delta \hat{a}_\psi) (\Delta \hat{a}_\psi \hat{S}_z) \rangle \right], \quad (38b)$$

$$\frac{d}{dt} \langle (\Delta \hat{S}_{-\psi-\pi/2})^2 \rangle = 2g \langle [\Delta \hat{S}_{-\psi-\pi/2}, \Delta \hat{a}_\psi \hat{S}_z]_+ \rangle, \quad (38c)$$

where  $\Delta \hat{O} \equiv \hat{O} - \langle \hat{O} \rangle$ , and  $[\hat{A}, \hat{B}]_+ \equiv \hat{A}\hat{B} + \hat{B}\hat{A}$  is an anti-commutator. The angle  $\psi$  in Eqs. (38) represents the direction of the fluctuations of the spin and the photon field, as shown in Fig. 7. The right-hand side of Eq. (38a) vanishes at  $t = 0$ , because initially the atoms and the photon field are not correlated. Since the first derivative vanishes at  $t = 0$ , the time development for small  $t$  is determined by the second derivative. From Eqs. (38a) and (38b) we have

$$\frac{d^2}{dt^2} \langle (\Delta \hat{a}_\psi)^2 \rangle = 2g^2 \left[ \langle (\Delta \hat{S}_{-\psi-\pi/2})^2 \rangle + 2 \langle (\Delta \hat{a}_\psi) (\Delta \hat{a}_\psi \hat{S}_z) \rangle \right]. \quad (39)$$

At  $t = 0$ , the right-hand side of Eq. (39) reduces to  $2g^2 [\langle (\Delta \hat{S}_{-\psi-\pi/2})^2 \rangle + \langle \hat{S}_z \rangle / 2]$  because  $\langle (\Delta \hat{a}_\psi)^2 \rangle = 1/4$  for the vacuum state. Therefore, if the initial spin state satisfies the condition,

$$\langle (\Delta \hat{S}_{-\psi-\pi/2})^2 \rangle < -\frac{\langle \hat{S}_z \rangle}{2}, \quad (40)$$

the photon field will evolve into a squeezed state. To satisfy the inequality (40),  $\langle \hat{S}_z \rangle$  must be negative. The equation of motion (39) indicates that the fluctuation profile of the photon field is connected with that of the spin state. From Eqs. (37a) and (39), then, the direction toward which the spin vector tilts corresponds to the direction of the displacement on the complex- $\alpha$  plane of the photon field, and the squeezed or enhanced direction of the spin fluctuation corresponds to that of the fluctuation of the photon field. Consequently, the quasi-probability distribution of the photon field on the complex- $\alpha$  plane is expected to behave like the quasi-probability distribution of the atoms on the spin sphere, as illustrated in Fig. 7.

When the tilting angle of the spin vector from the  $z$  axis is small, i.e.,  $\theta \simeq \pi$ , we can approximately solve the equations of motion (37) and (38). In this case,  $\langle \hat{S}_z \rangle$  is almost constant, and  $\hat{S}_z$  can be replaced by a constant c-number  $\langle \hat{S}_z \rangle_0$ , where  $\langle \cdots \rangle_0$  denotes the expectation value with respect to the initial state. With this approximation, Eqs. (37) can be solved, giving

$$\langle \hat{a}_\phi \rangle = \frac{\langle \hat{S}_{-\phi-\pi/2} \rangle_0}{\sqrt{2|\langle \hat{S}_z \rangle_0|}} \sin \sqrt{2|\langle \hat{S}_z \rangle_0|} gt, \quad (41a)$$

$$\langle \hat{S}_{-\phi-\pi/2} \rangle = \langle \hat{S}_{-\phi-\pi/2} \rangle_0 \cos \sqrt{2|\langle \hat{S}_z \rangle_0|} gt. \quad (41b)$$

The equations of motion for the fluctuations (38) become closed forms in this approximation, and the solutions are given by

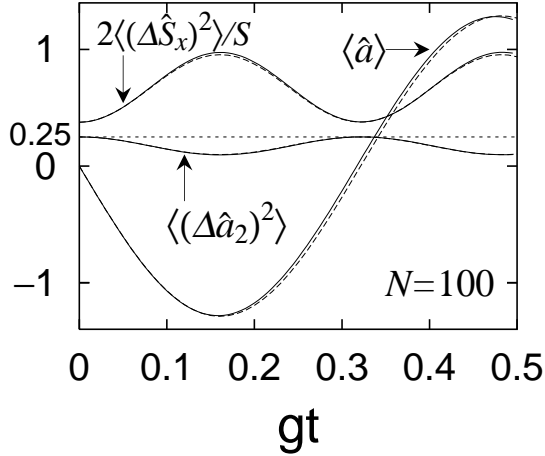


FIG. 8. Time evolutions of the normalized variance  $2\langle(\Delta\hat{S}_x)^2\rangle/S$  of the atoms, and the amplitude  $\langle\hat{a}\rangle$  and the variance  $\langle(\Delta\hat{a}_2)^2\rangle$  of the photon field emitted from them. The atomic state at  $gt = 0.14$  in Fig. 3 is used as the initial atom state. The field is initially in the vacuum state. The solid curves show the numerical solutions and the dashed curves show the approximate solutions (41a) and (42).

$$\begin{aligned} \langle(\Delta\hat{a}_\psi)^2\rangle = & \frac{1}{4} \cos^2 \sqrt{2|\langle\hat{S}_z\rangle_0|gt} \\ & + \frac{\langle(\Delta\hat{S}_{-\psi-\pi/2})^2\rangle_0}{2|\langle\hat{S}_z\rangle_0|} \sin^2 \sqrt{2|\langle\hat{S}_z\rangle_0|gt}, \end{aligned} \quad (42a)$$

$$\begin{aligned} \langle(\Delta\hat{S}_{-\psi-\pi/2})^2\rangle = & \langle(\Delta\hat{S}_{-\psi-\pi/2})^2\rangle_0 \cos^2 \sqrt{2|\langle\hat{S}_z\rangle_0|gt} \\ & + \frac{|\langle\hat{S}_z\rangle_0|}{2} \sin^2 \sqrt{2|\langle\hat{S}_z\rangle_0|gt}. \end{aligned} \quad (42b)$$

We find that if the condition (40) for the initial spin state is fulfilled, the variance of the quadrature amplitude (42a) goes below the SQL of  $1/4$ . At time  $t = \pi(2\sqrt{2|\langle\hat{S}_z\rangle_0|g})^{-1}$ , the fluctuation  $\langle(\Delta\hat{a}_\psi)^2\rangle$  attains its first minimum

$$\langle(\Delta\hat{a}_\psi)^2\rangle = \frac{\langle(\Delta\hat{S}_{-\psi-\pi/2})^2\rangle_0}{2|\langle\hat{S}_z\rangle_0|}, \quad (43)$$

and at the same time the amplitude of the field becomes maximum

$$\langle\hat{a}_\phi\rangle = \frac{\langle\hat{S}_{-\phi-\pi/2}\rangle_0}{\sqrt{2|\langle\hat{S}_z\rangle_0|}}. \quad (44)$$

Figure 8 shows time evolutions of the amplitude and the variance of the photon field, where the initial atomic state is the SAS of 100 atoms. This atomic state is prepared by the method discussed in Sec. IV (the

state at  $gt = 0.14$  in Fig. 3). Since the tilting angle  $\tan^{-1}(-\langle\hat{S}_y\rangle_0/\langle\hat{S}_z\rangle_0) = 0.258$  is small, the small-angle approximation is valid. The solutions (41) and (42) are used for the theoretical curves in Fig. 8 (dashed curves). One can see that the analytic results agree well with the numerical ones (solid curves), and  $\langle(\Delta\hat{a}_2)^2\rangle$  goes below the SQL of  $1/4$ . It can be shown numerically that the second and the later minimums of  $\langle(\Delta\hat{a}_2)^2\rangle$  are larger than the first minimum, and hence we should switch off the interaction when the first minimum is reached.

## B. Tailor-made radiation from squeezed atoms

As illustrated in Fig. 7, the quasi-probability distribution of the emitted photon state is like a projection from that of the prepared atomic state. This observation, together with the solutions (41) and (42), suggests to us that we can manipulate the direction of displacement and the direction of squeezing of photons by controlling the spin vector of the SAS. The rotation of the spin vector about an axis on the  $S_x$ - $S_y$  plane can be made by applying maser or laser with classical intensity to the atoms as described by the Hamiltonian (25). The rotation about the  $S_z$  axis is realized by applying a dc magnetic field which causes a temporal detuning by the Zeeman shift. Combining these two processes, we can manipulate both the spin vector and the direction of squeezing. By manipulating the SAS in the spin space, we can control the uncertainty ellipse of the photon field on the complex- $\alpha$  plane. Figure 9 shows the quasi-probability distributions of 100 atoms (left panels) and those of the emitted photon states (right panels). In Fig. 9(a) the CAS is used, and in Figs. 9(b)-(d) the atom states are prepared in the SASs by the method discussed in Sec. IV, where the parameters are optimized to obtain the maximum degree of spin squeezing ( $\alpha = 6.8$ ,  $gt = 0.19$ ). The tilting angle of the spin vector from the negative  $S_z$  axis is taken to be  $\pi/4$  in Figs. 9(a)-(d), and the uncertainty ellipses are turned around by  $0$ ,  $\pi/4$ , and  $\pi/2$  in Figs. 9(b), (c), and (d), respectively. One finds that the fluctuation profiles of the atomic states are rather faithfully transferred to those of the emitted photon states. Figures 9(c) and (d) suggest that not only amplitudes and fluctuations but also higher-order moments of atom states are transferred to those of the photon states. We have thus demonstrated that by manipulating the SAS, we can control quantum statistical properties of the photon field at our disposal, which we would like to call *tailor-made radiation*.

The squeezing of photons in the direction of phase can be obtained only if the atomic state is squeezed in the azimuth direction as in Fig. 9(b). Although the CAS can produce the photon-number squeezed state [31] as in Fig. 9(a), where the Fano factor is 0.81, it never produces the phase-squeezed photon state by any rotation on the spin sphere. This can be verified numerically, and

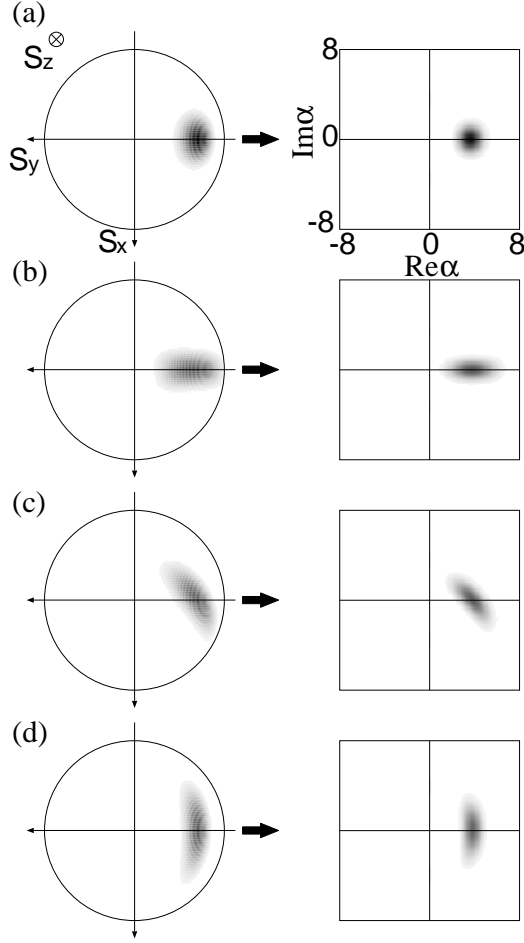


FIG. 9. The quasi-probability distributions of 100 atoms (left) and those of the photons emitted from the atoms (right). In (a) the atoms are prepared in a coherent atomic state, and in (b), (c), and (d), they are prepared in squeezed atom states. In (b), (c), and (d) the uncertainty ellipses are turned around by angles  $0$ ,  $\pi/4$ ,  $\pi/2$ , respectively. The mean spin vectors are tilted by  $\pi/4$  from the negative  $S_z$  axis. The spin sphere is seen from the negative  $S_z$  axis.

can also be deduced from the fact that the projection of the fluctuation profile on the complex- $\alpha$  plane from the spin sphere can never be squeezed in the direction of the phase if the fluctuation profile on the spin sphere is isotropic. To produce not only the amplitude-squeezed state but also the phase-squeezed state, the atom state must therefore be squeezed in the sense of the definition (23).

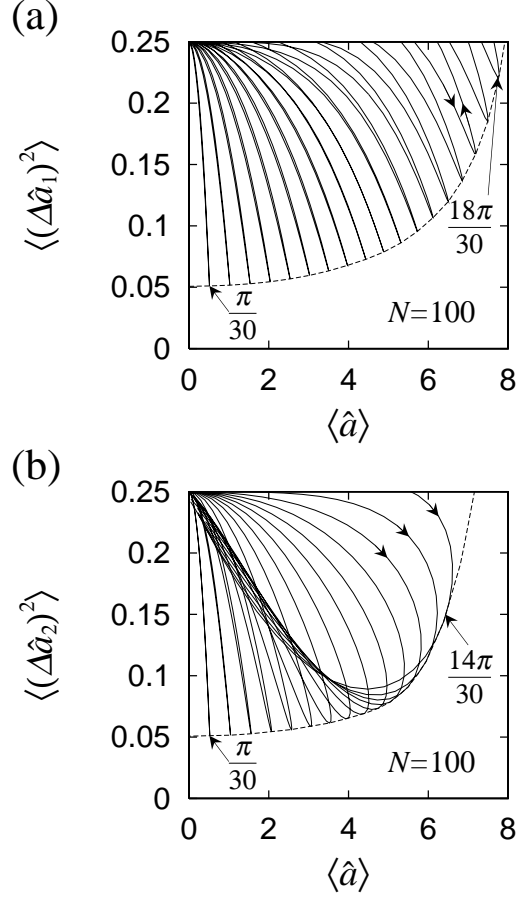


FIG. 10. Time evolution of the amplitudes and the variances of the quadrature components of the photon state emitted from the squeezed 100 atoms. Each trajectory is drawn with the initial tilting angle of the mean spin vector at every  $\pi/30$ . The squeezed atom states are prepared in the same manner as in Fig. 9 and rotated to the states which are squeezed in the latitudinal direction in (a) (as in Fig. 9(d)), and in the longitudinal direction in (b) (as in Fig. 9(b)). The dashed curves delimit the regions that the trajectories can reach.

### C. Available range of the tailor-made radiation

Let us discuss the range of photon squeezing that is available by our method. We use the SAS generated by the interaction between the totally excited atoms and the coherent state of the photon field with an optimum amplitude as discussed in Sec. IV. The available range of the emitted photon field is obtained by plotting time evolutions of the radiation processes for various initial tilting angles of the spin vector of the SAS.

Figure 10 shows time evolutions of the amplitudes and the variances of the quadrature amplitudes of the photon states emitted from the SASs of 100 atoms. Each

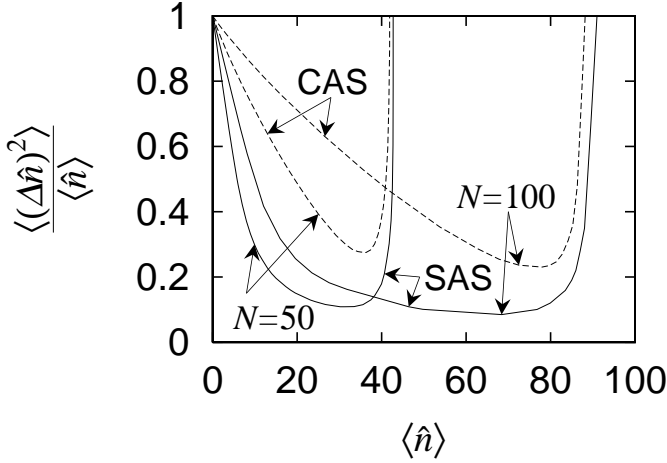


FIG. 11. Ranges of the average photon number  $\langle \hat{n} \rangle$  and the Fano factor  $\langle (\Delta \hat{n})^2 \rangle / \langle \hat{n} \rangle$  of the photon field that can be obtained by the squeezed atom state (SAS) and the coherent atom state (CAS) of 50 and 100 atoms. The SASs are prepared in the same manner as in Fig. 9. The regions above the curves show the available photon states. The solid curves show the results of the SASs and the dashed ones show those of the CASs.

trajectory is drawn with the initial tilting angle of the mean spin vector at every  $\pi/30$ . In Fig. 10(a), the SASs are prepared in the states squeezed in the longitudinal direction, as in Fig. 9(b). The emitted photon states are therefore out-of-phase squeezed states. In Fig. 10(b), the initial SASs are squeezed in the latitudinal direction as in Fig. 9(d), and the emitted photon states are therefore in-phase squeezed states. We find that in Fig. 10(a) the trajectories tend to return the same paths, whereas in Fig. 10(b) the trajectories tend to round downward. This indicates that in the case of in-phase squeezing the energy exchange and the fluctuation exchange between the atoms and the photon field tend to occur synchronously, and in the out-of-phase squeezing the fluctuation exchange tends to be delayed against the energy exchange. When we draw the overlap region of Figs. 10(a) and (b), we can obtain the available range of the quadrature-amplitude squeezed state. It can be shown that the larger number of atoms can produce the wider range of  $|\langle \hat{a} \rangle|$  and  $\langle (\Delta \hat{\phi})^2 \rangle$  [9]. This is due to the fact that the larger is the number of atoms the larger will be the degree of squeezing of the SAS, as shown in Fig. 6.

The ranges of the average photon number  $\langle \hat{n} \rangle$  and the Fano factor  $\langle (\Delta \hat{n})^2 \rangle / \langle \hat{n} \rangle$  available from the SASs and the CASs of 50 and 100 atoms are shown in Fig. 11. It is found that for a given number of atoms the SAS can suppress the photon-number fluctuation more effectively than the CAS. The range of 100 atoms does not cover that of 50 atoms in Fig. 11. The SAS of 50 atoms can

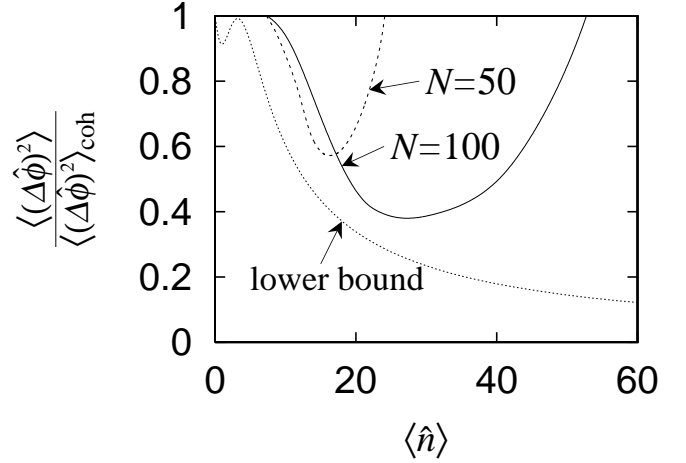


FIG. 12. Available ranges of the average photon number  $\langle \hat{n} \rangle$  and the phase fluctuation  $\langle (\Delta \hat{\phi})^2 \rangle$  normalized by that of the coherent state having the same average photon number  $\langle (\Delta \hat{\phi})^2 \rangle_{\text{coh}}$ . The regions above the curves show the photon states that can be obtained by our method. The squeezed atom states of 50 and 100 atoms are prepared in the same manner as in Fig. 9. The dotted curve shows the lower bound of  $\langle (\Delta \hat{\phi})^2 \rangle / \langle (\Delta \hat{\phi})^2 \rangle_{\text{coh}}$  of the photon field.

produce photon states having smaller Fano factors than the SAS of 100 atoms when the average photon number is less than about 40. For a given average photon number, therefore, there is an optimal number of atoms to produce the best photon-number squeezed state.

The ranges of the average photon number  $\langle \hat{n} \rangle$  and the phase fluctuation  $\langle (\Delta \hat{\phi})^2 \rangle$  available from the SASs of 50 and 100 atoms are shown in Fig. 12. Here we use the phase operator proposed by Pegg and Barnett [32]. When  $\langle \hat{a} \rangle$  is real and positive, the variance of the phase is expressed as

$$\langle (\Delta \hat{\phi})^2 \rangle = \frac{\pi^2}{3} + \sum_{n \neq n'} \frac{2(-1)^{n-n'}}{(n-n')^2} {}_F \langle n' | \hat{\rho}_F | n \rangle_F, \quad (45)$$

where  $\hat{\rho}_F$  is the density operator of the photon field and  $|n\rangle_F$  is the photon-number state. Figure 12 shows the variance of the phase  $\langle (\Delta \hat{\phi})^2 \rangle$  normalized by that of the coherent state having the same average photon number  $\langle (\Delta \hat{\phi})^2 \rangle_{\text{coh}}$ . Here the phase is defined as squeezed when  $\langle (\Delta \hat{\phi})^2 \rangle / \langle (\Delta \hat{\phi})^2 \rangle_{\text{coh}}$  is below unity. The dotted curve in Fig. 12 shows minimum values of  $\langle (\Delta \hat{\phi})^2 \rangle / \langle (\Delta \hat{\phi})^2 \rangle_{\text{coh}}$  for given average photon numbers, which are obtained by the method of Lagrange multipliers [33] (see appendix C). The range of 100 atoms does not completely include that of 50 atoms as in the case of the Fano factor, which indicates that for a given average photon number there is an optimal number of atoms to reduce the phase fluctuation.

In experimental situations, loss of photons in the cavity and spontaneous emission of atoms are unavoidable, and we therefore evaluate how much cavity loss and spontaneous emission are allowed in order not to destroy the squeezing of the atoms and that of the photon field. We adopt the master-equation approach to take into account the effects of dissipation. The master equation in the presence of cavity loss and spontaneous emission is given by [34]

$$\begin{aligned} \frac{\partial \hat{\rho}}{\partial t} = & \frac{i}{\hbar} [\hat{\rho}, \hat{H}^{\text{rot}}] + \frac{\gamma_f}{2} (2\hat{a}\hat{\rho}\hat{a}^\dagger - \hat{a}^\dagger\hat{a}\hat{\rho} - \hat{\rho}\hat{a}^\dagger\hat{a}) \\ & + \frac{\gamma_a}{2} (2\hat{S}_-\hat{\rho}\hat{S}_+ - \hat{S}_+\hat{S}_-\hat{\rho} - \hat{\rho}\hat{S}_+\hat{S}_-), \end{aligned} \quad (46)$$

where  $\hat{\rho}$  denotes the density operator of both the atoms and the photon field, and  $\gamma_f^{-1}$  and  $\gamma_a^{-1}$  are the lifetimes of a single photon and a single atom in the cavity. We obtain time evolution of the density operator by numerically integrating the master equation (46) by the Runge-Kutta method. Figure 13(a) shows the contour plot of the minimum attainable values of the squeezing factor  $2\langle(\Delta\hat{S}_x)^2\rangle/|\langle\hat{\mathbf{S}}\rangle|$  of the SASs obtained by the interaction of 10 atoms with the coherent state of the photon field. The amplitude of the coherent state is optimized to obtain the maximum degree of squeezing for each  $\gamma_f$  and  $\gamma_a$ . Figure 13(b) shows the contour plot of the minimum values of  $\langle(\Delta\hat{a}_\phi)^2\rangle$  of the photon field emitted from the squeezed atoms prepared in Fig. 13(a). The parameters  $\gamma_f$  and  $\gamma_a$  in the radiation process are assumed to have the same values as in the preparation of the SAS. These results show that the generation of the SAS and the squeezed radiation are possible even in the presence of dissipation in experimentally feasible situations. We will discuss some concrete numbers in the next section.

## VI. POSSIBLE EXPERIMENTAL SITUATIONS

We discuss possible experimental situations to implement our theory. Our procedure of generating quantum-controlled few-photon states consists of three stages: (1) preparation of the SAS, (2) manipulation of the SAS (rotation of the spin vector in the spin space), and (3) radiation from these atoms.

A simplest realization of our theory would be to fly a bunch of atoms through two cavities and a waveguide as schematically illustrated in Fig. 14. This type of experiment may be done in a microwave regime, since the atoms are required to be within a region much smaller than the wavelength. If we use, for example, the  $63\text{p}_{3/2} \leftrightarrow 61\text{d}_{3/2}$  transition of rubidium atoms, the resonant frequency is 21.5 GHz, the wavelength is  $\lambda \sim 10^{-2}$  m, and the coupling constant is  $g \sim 10^4$  Hz. First, an atomic beam from an oven is collimated and velocity-selected. The variance of the velocity of the atoms must be  $\Delta v \ll \lambda/T \sim 10^2$  m/s, where  $T$  is the time it takes the atoms to pass

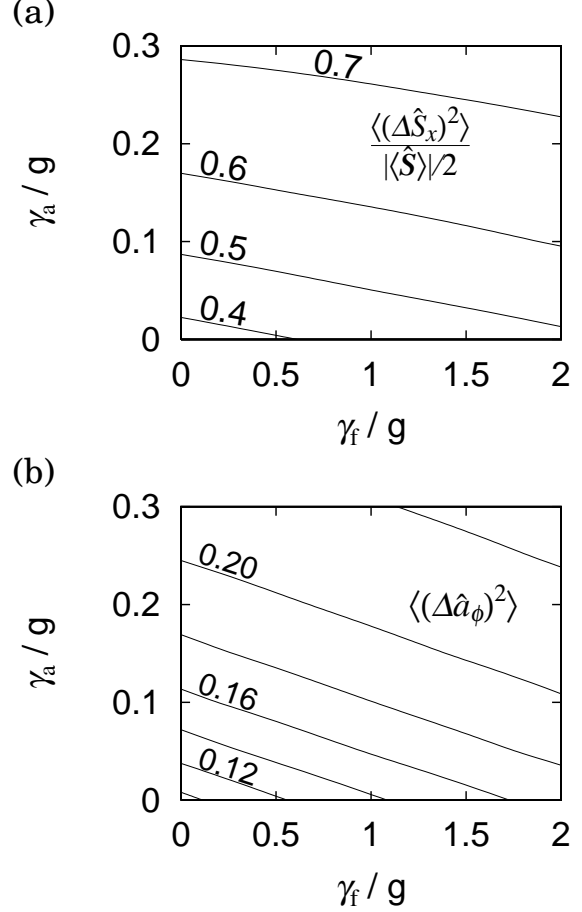


FIG. 13. (a) The contour plot of the minimum values of the squeezing factor  $2\langle(\Delta\hat{S}_x)^2\rangle/|\langle\hat{\mathbf{S}}\rangle|$  of the SASs obtained by the interaction of 10 atoms with the coherent state of the photon field. The amplitude of the coherent state is optimized to obtain the maximum degree of squeezing for each  $\gamma_f$  and  $\gamma_a$ . (b) The contour plot of the minimum values of  $\langle(\Delta\hat{a}_\phi)^2\rangle$  of the photon field emitted from the squeezed atoms prepared in (a).

through the apparatus. A mechanical shutter can prepare a bunch of atoms from the atomic beam. The atoms in the bunch are then excited to the Rydberg state that is the upper state of the relevant two-levels, and enter the first cavity in which the photon field is prepared to be in a coherent state  $|\alpha\rangle$ . The SAS is generated there by the higher-order interaction of the atoms with the coherent state. The interaction time is  $gt_1 \sim 10^{-1}$ , i.e.,  $t_1 \sim 10^{-5}$  s, e.g., in the situation in Fig. 4. The velocity of the atoms is therefore required to be  $v \sim 10^3$  m/s. The atoms then pass through a waveguide, where the atoms are irradiated by a pulse of microwave with classical intensity, by which the spin vector representing the state of collective atoms is rotated. To control the rotation axis of the spin vector, the relative phase between the microwave and the coherent state in the first cavity

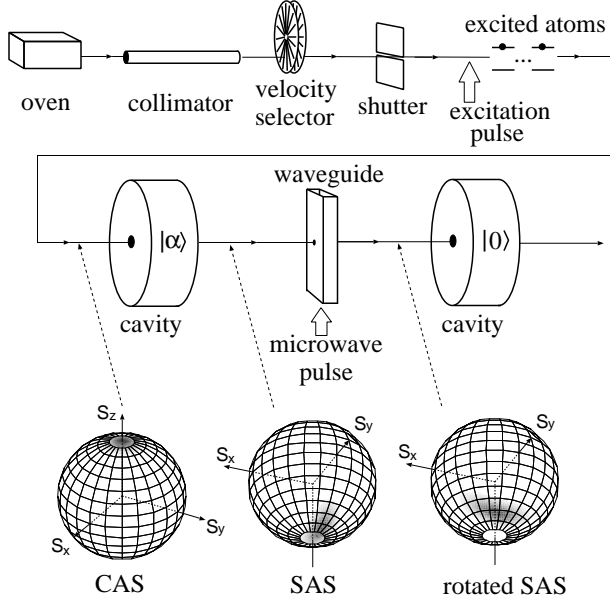


FIG. 14. Schematic illustration of an experimental setup to implement the tailor-made radiation. The state of the atoms at each stage is shown with the spin quasi-probability distribution. A bunch of two-level excited atoms that is in a coherent atom state (CAS) is prepared by an oven, a collimator, a velocity selector, a shutter, and a pulse that excites the atoms. The atoms then go into the first cavity and interact with a coherent state of the photon field  $|\alpha\rangle$ . The output atoms are in a squeezed atom state (SAS). By the interaction with a microwave pulse in a waveguide, the mean spin vector is rotated to a desired direction. The atoms finally go into the second cavity and emit photons there. Left in the second cavity is the desired few-photon state.

must be controlled. The irradiation time of the classical field is much shorter than the interaction time in both cavities. Finally, the atoms pass through the second cavity in which the desired state of photons is emitted from the atoms. The interaction time is  $gt_2 \sim 10^{-1}$ , i.e.,  $t_2 \sim 10^{-5}$ s, e.g., in the situation in Fig. 8. The atoms thus pass through the two cavities within a few periods of duration  $10^{-5}$ s, which is much shorter than the lifetime of the Rydberg atoms  $\sim 10^{-3}$ s and the cavity lifetime  $\sim 10^{-1}$ s [35]. From Fig. 13, this cavity lifetime corresponding to  $\gamma_f/g \sim 10^{-3}$  does not affect the squeezing. If the circular Rydberg states are used, the lifetime is  $\sim 1$  s, and decays from the relevant levels become negligible. Since the microwave frequency is used, the temperature should be lower than  $\sim 1$  K in order to make the average number of thermal photons in the cavity much smaller than that of the produced photons.

Another possible scheme is to use atoms confined in an ion trap or a magnetic trap in which the quantized kinetic motion of the atoms replaces the role of photons.

Wineland *et al.* [26] proposed the JC interaction between the Zeeman doublet of electronic states of each ion and the center-of-mass (CM) motion of an ensemble of ions via the inhomogeneous magnetic field. They pointed out that the stimulated Raman transition can also be used to couple the internal states of each ion to the CM motion of ions [26,36]. In these models the operators  $\hat{a}$  and  $\hat{a}^\dagger$  in the JC Hamiltonian (8) are not for photons but for the quantized CM motion of ions in a harmonic trap. By using the stimulated Raman technique, our theory might be implemented as follows. First, the internal levels of the trapped ions are excited and the CM motion is cooled to the ground state [37]. The CM motions of two orthogonal directions, say the  $z$  and  $x$  directions, correspond to the photon fields in the first and the second cavities in the method discussed in the preceding paragraph. In the first stage, the coherent state of the CM motion in the  $z$  direction is prepared and the Raman beams in this direction are applied. The coherent state of the CM motion can be generated by sudden displacement of the trap center. When the atomic internal state becomes the SAS, the Raman beams are switched off. In the second stage, the Raman beams that do not affect the CM motion are applied, which rotate the spin vector in the spin space. In the third stage, the Raman beams in the  $x$  direction are applied, and the internal states of the ions are coupled to the CM motion in the  $x$  direction. By this coupling the information of the internal states is transferred to the CM motion in the  $x$  direction, which may be called a tailor-made motional state. Although this is not radiation, the method using the trapped atoms might be used to test our theory.

The use of dielectric spheres as optical cavities might be another possibility, where the optical whispering gallery (WG) mode in the microsphere is employed. With the microsphere cavity, very low threshold lasing has been observed [38,39], and the Q value of more than  $10^9$  has been achieved with highly transparent silica glass optical-fiber material [40]. The atoms are fixed on the substrate and are coupled to evanescent waves of two microspheres which are placed very closely. They have the slightly different resonant frequencies  $\omega_1$  and  $\omega_2$ . The optical WG mode in the first microsphere is prepared in a coherent state, while that in the second one is prepared in the vacuum state. In the first stage, the atoms are brought into resonance with the WG mode frequency in the first microsphere  $\omega_1$ , and are far from resonant with that of the second microsphere  $\omega_2$ . This can be done by Zeeman-shifting the transition frequency of the atoms by a magnetic field. When the atomic state becomes the SAS by interacting with the coherent state, the interaction with the WG mode in the first microsphere is switched off by switching off the magnetic field. In the second stage, the spin vector is rotated by applying a laser pulse resonant with the transition frequency of the atoms. In the third stage, by applying an appropri-

ate magnetic field, the atoms are brought into resonance with the WG mode of the second microsphere  $\omega_2$ . By switching off the magnetic field, the desired photon state is left in the second microsphere. The coupling constant  $g$  can be of order  $10^8$ , and  $\gamma_f/g \sim 10^{-2}$  and  $\gamma_a/g \sim 10^{-1}$ , where the spontaneous emission rate of an atom in the free space is assumed. From Fig. 13, we find that both the SAS and the squeezed photon state are not washed out by the effects of dissipation.

## VII. CONCLUSIONS

In conclusion, we have shown that quantum fluctuations of few-photon states can be controlled by using the SAS. This controllability is based on the fact that quantum fluctuations of the atoms are faithfully transferred to those of the emitted photons. The correspondence shown in Fig. 9 between the quasi-probability distribution on the spin sphere and that on the complex- $\alpha$  plane indicates that a variety of photon states can be produced by merely rotating the spin vector of the SAS. We also found that this manipulation of few-photon states is possible only if the atoms are in the SAS. Although the CAS can produce the photon-number squeezed state, the degree of squeezing is lower than that of the photon state produced by the SAS, and the phase squeezed state can never be produced by the CAS. The possible experimental situations to implement our theory were discussed. By these schemes, we can generate the quantum-controlled few-photon state in the microcavity, and the quantum-controlled center-of-mass motion of trapped atoms.

## ACKNOWLEDGMENTS

One of the authors (H.S.) acknowledges support by a Research Fellowship of the Japan Society for the Promotion of Science for Young Scientists.

## APPENDIX A: VANISHING EXPECTATION VALUES IN THE JAYNES-CUMMINGS INTERACTION

It is assumed in Sec. IV that the expectation values  $\langle \hat{S}_x \rangle$  and  $\langle \hat{a}_2 \rangle$  always vanish if the time evolution is governed by the Hamiltonian (12) and when the initial state is  $|\alpha\rangle \otimes |S, M = S\rangle$  with real  $\alpha$ . In this appendix we give a general condition for this to be true.

Since an expectation value of an Hermitian operator, say  $\hat{O}$ , is real, it follows that

$$\begin{aligned} \langle e^{i\hat{H}^{\text{rot}}t} \hat{O} e^{-i\hat{H}^{\text{rot}}t} \rangle_0 &= \langle e^{i\hat{H}^{\text{rot}}t} \hat{O} e^{-i\hat{H}^{\text{rot}}t} \rangle_0^* \\ &= \langle e^{-i\hat{H}^{\text{rot}}t} \hat{O}^* e^{i\hat{H}^{\text{rot}}t} \rangle_0, \end{aligned} \quad (\text{A1})$$

where the expectation values are taken with respect to the initial state  $|\alpha\rangle \otimes |S, M = S\rangle$ , and  $\hat{O}^*$  denotes an operator whose matrix elements are complex conjugates of those of  $\hat{O}$ . In the second line of Eq. (A1) we used the fact that the matrix element of the Hamiltonian (12),

$$\begin{aligned} &\langle n | \langle S, M | \hat{H}^{\text{rot}} | S, M' \rangle | n' \rangle \\ &= g\hbar \left[ \sqrt{n+1} \sqrt{(S+M)(S-M+1)} \delta_{n,n'-1} \delta_{M,M'+1} \right. \\ &\quad \left. + \sqrt{n} \sqrt{(S-M)(S+M+1)} \delta_{n,n'+1} \delta_{M,M'-1} \right], \end{aligned} \quad (\text{A2})$$

is real and hence  $\hat{H}^{\text{rot}*} = \hat{H}^{\text{rot}}$ . By a unitary transformation  $e^{i\pi\hat{S}_z}$  we have  $e^{i\pi\hat{S}_z} \hat{H}^{\text{rot}} e^{-i\pi\hat{S}_z} = -\hat{H}^{\text{rot}}$  and  $e^{i\pi\hat{S}_z} |\alpha\rangle \otimes |S, M = S\rangle = e^{i\pi S} |\alpha\rangle \otimes |S, M = S\rangle$ . Applying this unitary transformation to the second line of (A1), the expectation value becomes

$$\langle e^{i\hat{H}^{\text{rot}}t} \hat{O} e^{-i\hat{H}^{\text{rot}}t} \rangle_0 = \langle e^{i\hat{H}^{\text{rot}}t} e^{i\pi\hat{S}_z} \hat{O}^* e^{-i\pi\hat{S}_z} e^{-i\hat{H}^{\text{rot}}t} \rangle_0. \quad (\text{A3})$$

Therefore, if  $e^{i\pi\hat{S}_z} \hat{O}^* e^{-i\pi\hat{S}_z} = -\hat{O}$ , the expectation value (A3) must vanish. The operators  $\hat{S}_x$  and  $\hat{a}_2$  meet this condition. In general, an expectation value of an Hermitian operator that consists of operator products in which  $\hat{S}_x$  and  $\hat{a}_2$  appear odd-numbered times always vanishes. General conditions required for the initial state of the photon field  $\hat{\rho}_F$  and that of the atoms  $\hat{\rho}_A$  are  $\hat{\rho}_F^* = \hat{\rho}_F$  and  $e^{i\pi\hat{S}_z} \hat{\rho}_A e^{-i\pi\hat{S}_z} = \hat{\rho}_A$ .

## APPENDIX B: DERIVATION OF THE APPROXIMATE SOLUTIONS (35)

In this appendix, we derive the approximate solutions (35). It is convenient to define [31]

$$\hat{a}'_i \equiv \frac{\hat{a}_i}{\sqrt{N}} \quad (i = 1, 2), \quad (\text{B1a})$$

$$\hat{S}'_\mu \equiv \frac{\hat{S}_\mu}{N} \quad (\mu = x, y, z), \quad (\text{B1b})$$

$$\tau \equiv g\sqrt{N}t, \quad (\text{B1c})$$

in order to estimate errors of the approximation. The equations of motion for these operators have the forms

$$\partial_\tau \hat{S}'_x = -2\hat{a}'_2 \hat{S}'_z, \quad (\text{B2a})$$

$$\partial_\tau \hat{S}'_y = -2\hat{a}'_1 \hat{S}'_z, \quad (\text{B2b})$$

$$\partial_\tau \hat{S}'_z = 2(\hat{a}'_1 \hat{S}'_y + \hat{a}'_2 \hat{S}'_x), \quad (\text{B2c})$$

$$\partial_\tau \hat{a}'_1 = -\hat{S}'_y, \quad (\text{B2d})$$

$$\partial_\tau \hat{a}'_2 = -\hat{S}'_x. \quad (\text{B2e})$$

We assume that the initial state is the CAS  $|\theta = 0, \phi\rangle$  for the atoms and the coherent state  $|\alpha\rangle$  for the photon field,



where  $\alpha$  is taken to be real without loss of generality. Taking the expectation values of Eqs. (B2) yields

$$\partial_\tau \langle \hat{S}'_y \rangle = -2\langle \hat{a}'_1 \rangle \langle \hat{S}'_z \rangle - 2\langle \Delta \hat{a}'_1 \Delta \hat{S}'_z \rangle, \quad (\text{B3a})$$

$$\partial_\tau \langle \hat{S}'_z \rangle = 2\langle \hat{a}'_1 \rangle \langle \hat{S}'_y \rangle - 2\langle \Delta \hat{a}'_1 \Delta \hat{S}'_y \rangle, \quad (\text{B3b})$$

$$\partial_\tau \langle \hat{a}'_1 \rangle = -\langle \hat{S}'_y \rangle, \quad (\text{B3c})$$

where  $\Delta \hat{O} \equiv \hat{O} - \langle \hat{O} \rangle$  for any operators. It can be shown that  $\langle \hat{S}'_y \rangle$ ,  $\langle \hat{S}'_z \rangle$ , and  $\langle \hat{a}'_1 \rangle$  are of order unity, and  $\langle \Delta \hat{a}'_1 \Delta \hat{S}'_z \rangle$  and  $\langle \Delta \hat{a}'_1 \Delta \hat{S}'_y \rangle$  are of order  $1/N$ . If we neglect relative errors of  $1/N$ , the second terms of Eqs. (B3a) and (B3b) can be neglected, giving

$$\partial_\tau \langle \hat{S}'_y \rangle = -2\langle \hat{a}'_1 \rangle \langle \hat{S}'_z \rangle, \quad (\text{B4a})$$

$$\partial_\tau \langle \hat{S}'_z \rangle = 2\langle \hat{a}'_1 \rangle \langle \hat{S}'_y \rangle, \quad (\text{B4b})$$

$$\partial_\tau \langle \hat{a}'_1 \rangle = -\langle \hat{S}'_y \rangle. \quad (\text{B4c})$$

If we set

$$\langle \hat{S}'_y \rangle = \frac{1}{2} \sin \theta(\tau), \quad (\text{B5a})$$

$$\langle \hat{S}'_z \rangle = \frac{1}{2} \cos \theta(\tau), \quad (\text{B5b})$$

$$\langle \hat{a}'_1 \rangle = -\frac{1}{2} \partial_\tau \theta(\tau), \quad (\text{B5c})$$

the equations of motion (B3) reduce to

$$\partial_\tau^2 \theta(\tau) = \sin \theta(\tau), \quad (\text{B6})$$

which has the same form as the equation of motion for the mechanical pendulum. The angular velocity of the pendulum corresponds to the field amplitude. The solutions for the initial condition  $\theta(0) = 0$  and  $\partial_\tau \theta(0) = -2\alpha'$ , where  $\alpha' \equiv \alpha/\sqrt{N}$ , can be expressed in terms of Jacobi's elliptic functions as

$$\langle \hat{S}'_y \rangle = -\sqrt{1-m} \text{sd}(u|m) \text{cd}(u|m), \quad (\text{B7a})$$

$$\langle \hat{S}'_z \rangle = \frac{1}{2} [2\text{cd}^2(u|m) - 1], \quad (\text{B7b})$$

$$\langle \hat{a}'_1 \rangle = \alpha' \text{nd}(u|m), \quad (\text{B7c})$$

$$\langle \hat{a}'_1 \rangle = \langle \hat{S}'_x \rangle = 0, \quad (\text{B7d})$$

where  $u \equiv \tau\sqrt{1+\alpha'^2}$  and  $m \equiv 1/(1+\alpha'^2)$ .

The equations of motion for variances are written as

$$\partial_\tau \langle (\Delta \hat{a}'_2)^2 \rangle = -2\langle \Delta \hat{a}'_2 \Delta \hat{S}'_x \rangle, \quad (\text{B8a})$$

$$\begin{aligned} \partial_\tau \langle (\Delta \hat{S}'_x)^2 \rangle &= -4\langle \Delta \hat{a}'_2 \Delta \hat{S}'_x \rangle \langle \hat{S}'_z \rangle + 2\langle \Delta \hat{S}'_x \Delta \hat{S}'_z \Delta \hat{a}'_2 \rangle \\ &\quad + 2\langle \Delta \hat{S}'_z \Delta \hat{S}'_x \Delta \hat{a}'_2 \rangle, \end{aligned} \quad (\text{B8b})$$

$$\begin{aligned} \partial_\tau \langle \Delta \hat{a}'_2 \Delta \hat{S}'_x \rangle &= -\langle (\Delta \hat{S}'_x)^2 \rangle - \langle (\Delta \hat{a}'_2)^2 \rangle \langle \hat{S}'_z \rangle \\ &\quad - \langle (\Delta \hat{a}'_2)^2 \Delta \hat{S}'_z \rangle. \end{aligned} \quad (\text{B8c})$$

It can be shown that the second-order fluctuations, such as  $\langle (\Delta \hat{S}'_x)^2 \rangle$ , are of order  $1/N$ , and that the third-order fluctuations, such as  $\langle \Delta \hat{S}'_x \Delta \hat{S}'_z \Delta \hat{a}'_2 \rangle$ , are of order  $1/N^2$ .

Neglecting the third-order fluctuations in Eqs. (B8), we have

$$\partial_\tau \langle (\Delta \hat{a}'_2)^2 \rangle = -2\langle \Delta \hat{a}'_2 \Delta \hat{S}'_x \rangle, \quad (\text{B9a})$$

$$\partial_\tau \langle (\Delta \hat{S}'_x)^2 \rangle = -4\langle \Delta \hat{a}'_2 \Delta \hat{S}'_x \rangle \langle \hat{S}'_z \rangle, \quad (\text{B9b})$$

$$\partial_\tau \langle \Delta \hat{a}'_2 \Delta \hat{S}'_x \rangle = -\langle (\Delta \hat{S}'_x)^2 \rangle - \langle (\Delta \hat{a}'_2)^2 \rangle \langle \hat{S}'_z \rangle. \quad (\text{B9c})$$

Using the form of  $\langle \hat{S}'_z \rangle$  in Eq. (B7b), which has at most a relative error of  $1/N$ , Eqs. (B8) reduce to the closed differential equations with relative errors  $1/N$ . They have three independent sets of solutions, and two of them are obtained as

$$\begin{pmatrix} \langle (\Delta \hat{a}'_2)^2 \rangle \\ \langle (\Delta \hat{S}'_x)^2 \rangle \\ \langle \Delta \hat{a}'_2 \Delta \hat{S}'_x \rangle \end{pmatrix} = \begin{pmatrix} \frac{1}{N} \text{nd}^2(u|m) \\ \frac{m}{N} \text{sd}^2(u|m) \text{cd}^2(u|m) \\ -\frac{\sqrt{m}}{N} \text{sd}(u|m) \text{cd}(u|m) \text{nd}(u|m) \end{pmatrix}, \quad (\text{B10})$$

$$\begin{pmatrix} \frac{1}{N} \text{nd}^2(u|m) E^2(u|m) \\ \frac{m}{N} [m \text{sd}(u|m) \text{cd}(u|m) E(u|m) + \text{dn}(u|m)]^2 \\ -\frac{\sqrt{m}}{N} [m \text{sd}(u|m) \text{cd}(u|m) E(u|m) + \text{dn}(u|m)] \text{nd}(u|m) E(u|m) \end{pmatrix}.$$

The linear combination of these solutions to satisfy the initial conditions  $\langle (\Delta \hat{S}'_x)^2 \rangle = \frac{1}{4N}$ ,  $\langle (\Delta \hat{a}'_2)^2 \rangle = \frac{1}{4N}$ , and  $\langle \Delta \hat{a}'_2 \Delta \hat{S}'_x \rangle = 0$  yields the solutions (35).

### APPENDIX C: A METHOD TO MINIMIZE THE PHASE FLUCTUATION

In this appendix, we briefly show a method to obtain a photon state having the minimum phase fluctuation, which is the dotted curve in Fig. 12. The variance of the Pegg-Barnett phase operator of the photon state  $\sum_n c_n |n\rangle_F$  is given by

$$\langle (\Delta \hat{\phi})^2 \rangle = \frac{\pi^2}{3} + 2 \sum_{n \neq m} A_{nm} c_n c_m, \quad (\text{C1})$$

where  $A_{nm} = (-1)^{n-m}/(n-m)^2$ . The coefficients that minimize the variance (C1) satisfying the constraints  $\sum_n c_n^2 = 1$  and  $\sum_n n c_n^2 = \bar{n}$  are obtained by minimizing the function

$$\begin{aligned} F(\{c_n\}, \lambda, \beta) &= 2 \sum_{n \neq m} A_{nm} c_n c_m + \lambda \left( \sum_n c_n^2 - 1 \right) \\ &\quad + \beta \left( \sum_n n c_n^2 - \bar{n} \right), \end{aligned} \quad (\text{C2})$$

where  $\lambda$  and  $\beta$  are the Lagrange multipliers. The variational problem  $\partial F / \partial c_n = 0$  is equivalent to the eigenvalue problem

$$\sum_{n'} (2A_{nn'} + n\beta \delta_{nn'}) c_{n'} + \lambda c_n = 0, \quad (\text{C3})$$

which can be solved numerically.

- 
- [1] For collections of review articles, see, for example, R. Loudon and P. L. Knight (eds), *J. Mod. Opt.* **34**, (6/7) (1987); H. J. Kimble and D. F. Walls (eds), *J. Opt. Soc. Am. B* **4**, (10) (1987).
  - [2] For reviews, see, for example, H. J. Kimble, *Phys. Rep.* **219**, 227 (1992); in *Fundamental Systems in Quantum Optics* (Elsevier, Amsterdam, 1992), p. 545.
  - [3] R. E. Slusher, L. W. Hollberg, B. Yurke, J. C. Mertz and J. F. Valley, *Phys. Rev. Lett.* **55**, 2409 (1985).
  - [4] L. A. Wu, H. J. Kimble, J. L. Hall, and H. Wu, *Phys. Rev. Lett.* **57**, 2520 (1986); E. S. Polzik, J. Carri, and H. J. Kimble, *Phys. Rev. Lett.* **68**, 3020 (1992).
  - [5] S. Machida, Y. Yamamoto, and Y. Itaya, *Phys. Rev. Lett.* **58**, 1000 (1987).
  - [6] P. R. Tapster, J. G. Rarity, and J. S. Satchell, *Europhys. Lett.* **4**, 293 (1987).
  - [7] T. Hirano and T. Kuga, *IEEE J. Quant. Elec.* **31**, 2236 (1995).
  - [8] M. Yamanishi, K. Watanabe, N. Jikutani, and M. Ueda, *Phys. Rev. Lett.* **76**, 3432 (1996).
  - [9] H. Saito and M. Ueda, *Phys. Rev. Lett.* **79**, 3869 (1997).
  - [10] L. Allen and J. H. Eberly, *Optical Resonances and Two-level Atoms* (Dover, New York, 1987).
  - [11] R. H. Dicke, *Phys. Rev.* **93**, 99 (1954).
  - [12] B. R. Mollow, in *Progress in Optics XIX*, edited by E. Wolf (North-Holland, Amsterdam, 1981).
  - [13] D. Meschede, H. Walther, and G. Müller, *Phys. Rev. Lett.* **54**, 551 (1985).
  - [14] H. J. Carmichael and D. F. Walls, *J. Phys. B* **9**, 1199 (1976).
  - [15] H. J. Kimble, M. Dagenais, and L. Mandel, *Phys. Rev. Lett.* **39**, 691 (1977).
  - [16] D. F. Walls and P. Zoller, *Phys. Rev. Lett.* **47**, 709 (1981).
  - [17] J. M. Radcliffe, *J. Phys. A* **4**, 313 (1971); F. T. Arecchi, E. Courtens, R. Gilmore, and H. Thomas, *Phys. Rev. A* **6**, 2211 (1972).
  - [18] M. Ueda, T. Wakabayashi, and M. Kuwata-Gonokami, *Phys. Rev. Lett.* **76**, 2045 (1996).
  - [19] K. Wódkiewicz, *Opt. Commun.* **51**, 198 (1984); *Phys. Rev. B* **32**, 4750 (1985); K. Wódkiewicz and J. H. Eberly, *J. Opt. Soc. Am. B* **2**, 458 (1985); K. Wódkiewicz, P. L. Knight, S. J. Buckle, and S. M. Barnett, *Phys. Rev. A* **35**, 2567 (1987).
  - [20] J. D. Macomber and R. Lynch, *J. Chem. Phys.* **83**, 6514 (1985).
  - [21] B. Yurke, *Phys. Rev. Lett.* **56**, 1515 (1986); B. Yurke, S. L. McCall, and J. R. Klauder, *Phys. Rev. A* **33**, 4033 (1986).
  - [22] P. K. Aravind, *J. Opt. Soc. Am. B* **3**, 1545 (1986).
  - [23] S. M. Barnett and M. -A. Dupertuis, *J. Opt. Soc. Am. B* **4**, 505 (1987).
  - [24] G. S. Agarwal and R. R. Puri, *Phys. Rev. A* **41**, 3782 (1990).
  - [25] M. Kitagawa and M. Ueda, *Phys. Rev. Lett.* **67**, 1852 (1991); *Phys. Rev. A* **47**, 5138 (1993).
  - [26] D. J. Wineland, J. J. Bollinger, W. M. Itano, F. L. Moore, and D. J. Heinzen, *Phys. Rev. A* **46**, R6797 (1992); D. J. Wineland, J. J. Bollinger, W. M. Itano, and D. J. Heinzen, *Phys. Rev. A* **50**, 67 (1994).
  - [27] E. Jaynes and F. Cummings, *Proc. IEEE* **51**, 89 (1963); M. Tavis and F. W. Cummings, *Phys. Rev.* **170**, 379 (1968); for a recent review of the Jaynes-Cummings model, see B. W. Shore and P. L. Knight, *J. Mod. Opt.* **40**, 1195 (1993).
  - [28] A. Kuzmich, K. Mølmer, and E. S. Polzik, *Phys. Rev. Lett.* **79**, 4782 (1997).
  - [29] *Handbook of Mathematical Functions*, edited by M. Abramowitz and I. A. Stegun (Dover, New York, 1969).
  - [30] J. H. Eberly, N. B. Narozhny, and J. J. Sanchez-Mondragon, *Phys. Rev. Lett.* **44**, 1323 (1980).
  - [31] A. Heidmann, J. M. Raimond, and S. Reynaud, *Phys. Rev. Lett.* **54**, 326 (1985). A. Heidmann, J. M. Raimond, S. Reynaud, and N. Zagury, *Opt. Commun.* **54**, 189 (1985).
  - [32] D. T. Pegg and S. M. Barnett, *Europhys. Lett.* **6**, 483 (1988); *J. Mod. Opt.* **36**, 7 (1989). S. M. Barnett and D. T. Pegg, *Phys. Rev. A* **39**, 1665 (1989).
  - [33] G. M. D'Ariano and M. G. A. Paris, *Phys. Rev. A* **49**, 3022 (1994).
  - [34] W. H. Louisell, *Quantum Statistical Properties of Radiation*, (Wiley, New York, 1973).
  - [35] G. Rempe, F. Schmidt-Kaler, and H. Walther, *Phys. Rev. Lett.* **64**, 2783 (1990).
  - [36] D. J. Heinzen and D. J. Wineland, *Phys. Rev. A* **42**, 2977 (1990).
  - [37] F. Diedrich, J. C. Bergquist, W. M. Itano, and D. J. Wineland, *Phys. Rev. Lett.* **62**, 403 (1989).
  - [38] H. M. Tseng, K. F. Wall, M. B. Long, and R. K. Chang, *Opt. Lett.* **9**, 499 (1984).
  - [39] M. Kuwata-Gonokami, K. Takeda, H. Yasuda, and K. Ema, *Jpn. J. Appl. Phys.* **31**, L99 (1992).
  - [40] L. Collot, V. Lefevre-Sguin, M. Brune, J. M. Raimond, and S. Haroche, *Europhys. Lett.* **23**, 327 (1993).